

A Boussinesq system for two-way propagation of interfacial waves

Hai Yen Nguyen, Frédéric Dias ^a

^a*CMLA, ENS Cachan, CNRS, PRES UniverSud, 61, avenue du Président Wilson, 94230 Cachan cedex, France*

Abstract

The theory of internal waves between two layers of immiscible fluids is important both for its applications in oceanography and engineering, and as a source of interesting mathematical model equations that exhibit nonlinearity and dispersion. A Boussinesq system for two-way propagation of interfacial waves in a rigid lid configuration is derived. In most cases, the nonlinearity is quadratic. However, when the square of the depth ratio is close to the density ratio, the coefficients of the quadratic nonlinearities become small and cubic nonlinearities must be considered. The propagation as well as the collision of solitary waves and/or fronts is studied numerically.

1 Introduction

As emphasized by Helfrich & Melville [20] in their recent survey article on long nonlinear internal waves, observations over the past four decades have demonstrated that internal solitary-like waves are ubiquitous features of coastal oceans and marginal seas. Solitary waves are long nonlinear waves consisting of a localized central core and a decaying tail. They arise whenever there is a balance between dispersion and nonlinearity. They have been proved to exist in specific parameter regimes, and are often conveniently modelled by Korteweg–de Vries (KdV) equations or Boussinesq systems. As explained by Evans & Ford [16], the differences between “free-surface” and “rigid lid” internal waves are small for internal waves of interest. Therefore the “rigid lid” configuration remains popular for investigating internal waves even if it does not allow for generalized solitary waves, which are long nonlinear waves consisting of a localized central core and periodic non-decaying oscillations extending to infinity. Such waves arise whenever there is a resonance between a linear long wave speed of one wave mode in the system and a linear short wave speed of another mode [17].

When dealing with interfacial waves with rigid boundaries in the framework of the full Euler equations, the amplitude of the central core is bounded by the configuration. In the case of solitary waves, it is known that when the wave speed approaches a critical value the solution reaches a maximum amplitude while becoming indefinitely wider; these waves are often called ‘table-top’ waves. In the limit as the width of the central core becomes infinite, the wave becomes a front [13]. Such behavior is conveniently modelled by an extended Korteweg–de Vries (eKdV) equation, i.e. a KdV equation with a cubic nonlinear term [18]. Sometimes the terminology ‘modified KdV equation’ or ‘Gardner equation’ is also used. KdV-type equations only describe one-way wave propagation. The natural extension toward two-way wave propagation is the class of Boussinesq systems. We will derive two sets of Boussinesq systems, one with quadratic nonlinearities and another one with quadratic and cubic nonlinearities. We will use the terminology ‘extended’ for a Boussinesq system with both quadratic and cubic terms. Some questions arise when dealing with ‘table-top’ solitary waves. What are their properties? How do they interact? The main goal of this work is to learn more about these waves by studying and integrating numerically an extended Boussinesq system which allows a comparison between fronts and the more standard solitary waves. More general models have also been derived by Choi & Camassa [9]. They considered shallow water as well as deep water configurations. In the shallow water case, their set of equations is the two-layer version of the Green–Naghdi equations. The equations derived in [9] were recently extended to the free-surface configuration [2]. Solitary waves for two-layer flows have also been computed numerically as solutions to the full incompressible Euler equations in the presence of an interface by various authors – see for example [22]. Similarly fronts have been computed for example in [13,14].

The paper is organized as follows. In § 2, we present the governing equations and the corresponding boundary conditions. A first Boussinesq system of three equations is derived in § 3. Then it is shown in § 4 how to reduce this system to a system of two equations, one for the evolution of the interface shape and the other one for the evolution of a combination of the horizontal velocities in each layer. The numerical scheme and the numerical solutions are described in § 5. Results are shown for the propagation of a single wave, for the co-propagation of two waves and for the collision of two waves of equal as well as unequal sizes. When the square of the depth ratio is close to the density ratio, the coefficients of the quadratic nonlinearities become small and cubic nonlinearities must be considered. An extended Boussinesq system is derived in § 6. Numerical solutions of the extended Boussinesq system are described in § 7. In particular, the collision of ‘table-top’ waves is considered. A short conclusion is given in § 8. In the Appendices, we provide very accurate results for wave run-up and phase shift, as well as some intermediate steps in the derivation of the extended Boussinesq system.

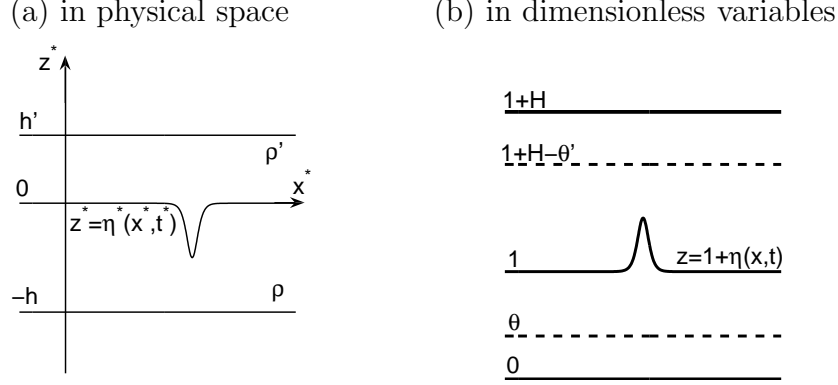


Fig. 1. Sketch of solitary waves propagating at the interface between two fluid layers with different densities ρ' and ρ . The top and the bottom of the fluid domain are flat and rigid boundaries, located respectively at $z^* = h'$ and $z^* = -h$. (a) Sketch of a solitary wave of depression in physical space; (b) Sketch of a solitary wave of elevation in dimensionless coordinates, with the thickness h of the bottom layer taken as unit length and the long wave speed c as unit velocity. The dashed lines represent arbitrary fluid levels θ and $1 + H - \theta'$ in each layer. The dimensionless number H is equal to h'/h .

2 Governing equations

The origin of the systems of partial differential equations that will be derived below is explained in this section. The methods are standard, but to our knowledge some of these equations are derived for the first time.

Waves at the interface between two fluids are considered. The bottom as well as the upper boundary are assumed to be flat and rigid. A sketch is given in Figure 1. The analysis is restricted to two-dimensional flows. In other words, there is only one horizontal direction, x^* , in addition to the vertical direction, z^* . The interface is described by $z^* = \eta^*(x^*, t^*)$. The bottom layer $\Omega_{t^*} = \{(x^*, z^*) : x^* \in \mathbb{R}, -h < z^* < \eta^*(x^*, t^*)\}$ and the upper layer $\Omega'_{t^*} = \{(x^*, z^*) : x^* \in \mathbb{R}, \eta^*(x^*, t^*) < z^* < h'\}$ are filled with inviscid, incompressible fluids, with densities ρ and ρ' respectively. All quantities related to the upper layer are denoted with a prime. All physical variables are denoted with a star.

In addition the flows are assumed to be irrotational. Therefore we are dealing with potential flows and only stable configurations with $\rho > \rho'$ are considered. Velocity potentials $\phi^* = \phi^*((x^*, z^*), t^*)$ in Ω_{t^*} and $\phi^{*'} = \phi^{*'}((x^*, z^*), t^*)$ in Ω'_{t^*} are introduced, so that the velocity vectors \mathbf{v}^* and $\mathbf{v}^{*'}$ are given by

$$\mathbf{v}^* = \nabla \phi^*, \quad (1)$$

$$\mathbf{v}^{*' } = \nabla \phi^{*'}. \quad (2)$$

Writing the continuity equations in each layer leads to

$$\phi_{x^*x^*}^* + \phi_{z^*z^*}^* = 0 \quad \text{for } -h < z^* < \eta^*(x^*, t^*), \quad (3)$$

$$\phi_{x^*x^*}' + \phi_{z^*z^*}' = 0 \quad \text{for } \eta^*(x^*, t^*) < z^* < h'. \quad (4)$$

The boundary of the system $\{\Omega_{t^*}, \Omega'_{t^*}\}$ has two parts: the flat bottom $z^* = -h$ and the flat roof $z^* = h'$. The impermeability conditions along these rigid boundaries give

$$\phi_{z^*}^* = 0 \quad \text{at } z^* = -h, \quad (5)$$

$$\phi_{z^*}' = 0 \quad \text{at } z^* = h'. \quad (6)$$

The kinematic conditions along the interface, namely $D(\eta^* - z^*)/Dt^* = 0$, give

$$\eta_{t^*}^* = \phi_{z^*}^* - \phi_x^* \eta_x^* \quad \text{at } z^* = \eta^*(x^*, t^*), \quad (7)$$

$$\eta_{t^*}' = \phi_{z^*}' - \phi_x' \eta_x^* \quad \text{at } z^* = \eta^*(x^*, t^*). \quad (8)$$

The dynamic boundary condition imposed on the interface, namely the continuity of pressure since surface tension effects are neglected, gives

$$\rho \left(\frac{\partial \phi^*}{\partial t^*} + \frac{1}{2} |\nabla \phi^*|^2 + g z^* \right) = \rho' \left(\frac{\partial \phi'}{\partial t^*} + \frac{1}{2} |\nabla \phi'|^2 + g z^* \right) \quad \text{at } z^* = \eta^*(x^*, t^*), \quad (9)$$

where g is the acceleration due to gravity. The system of seven equations (3)–(9) represents the starting model for the study of wave propagation at the interface between two fluids. Combined with initial conditions or periodicity conditions, it is the classical interfacial wave problem, which has been studied for more than a century. A nice feature of this formulation is that the pressures in both layers have been removed. In some cases, it is advantageous to keep the pressures in the equations. For example, Bridges & Donaldson [8] in their study of the criticality of two-layer flows provide an appendix on the inclusion of the lid pressure in the calculation of uniform flows. In the next sections, we will derive simplified models based on certain additional assumptions on wave amplitude, wavelength and fluid depth.

3 System of three equations in the limit of long, weakly dispersive waves

The derivation follows closely that of [5] for a single layer. Let us now consider waves whose typical amplitude, A , is small compared to the depth of the

bottom layer h , and whose typical wavelength, ℓ , is large compared to the depth of the bottom layer¹. Let us define the three following dimensionless numbers, with their characteristic magnitude:

$$\alpha = \frac{A}{h} \ll 1, \quad \beta = \frac{h^2}{\ell^2} \ll 1, \quad S = \frac{\alpha}{\beta} = \frac{A\ell^2}{h^3} \approx 1.$$

Here S is the Stokes number. Let us also introduce the dimensionless density ratio r as well as the depth ratio H :

$$r = \frac{\rho'}{\rho}, \quad H = \frac{h'}{h}.$$

Obviously r takes values between 0 and 1, the case $r = 0$ corresponding to water waves² while the case $r \approx 1$ corresponds to two fluids with almost the same density such as an upper, warmer layer extending down to the interface with a colder, more saline layer. The depth ratio takes theoretical values between 0 and ∞ but as said above values $H \ll 1$ or $H \gg 1$ should be avoided in the framework of our weakly nonlinear analysis.

The procedure is most transparent when working with the variables scaled in such a way that the dependent quantities appearing in the problem are all of order one, while the assumptions about small amplitude and long wavelength appear explicitly connected with small parameters in the equations of motion. Such consideration leads to the scaled, dimensionless variables

$$x^* = \ell x, \quad z^* = h(z-1), \quad \eta^* = A\eta, \quad t^* = \ell t/c_0, \quad \phi^* = gA\ell\phi/c_0, \quad \phi^{*'} = gA\ell\phi'/c_0,$$

where $c_0 = \sqrt{gh}$. The speed c_0 , which represents the long wave speed in the limit $r \rightarrow 0$, is not necessarily the most natural choice for interfacial waves. The natural choice would be to take

$$c_0 = \sqrt{gh} \sqrt{\frac{1-r}{1+r/H}},$$

which is the speed of long waves in the configuration shown in Figure 1. It does not matter for the asymptotic expansions to be performed later.

¹ There is some arbitrariness in this choice since there are two fluid depths in the problem. We could have also chosen the depth of the top layer as reference depth. In fact, we implicitly make the assumption that the ratio of liquid depths is neither too small nor too large, without going into mathematical details. Models valid for arbitrary depth ratio have been derived for example by Choi & Camassa [9].

² In a recent paper, Kataoka [21] showed that when H is near unity, the stability of solitary waves changes drastically for small density ratios r . Therefore one must be careful in evaluating the stability of air-water solitary waves. In other words, there may be differences between $r = 0$ and the true value $r = 0.0013$.

In these new variables, the set of equations (3)–(9) becomes after reordering

$$\beta\phi_{xx} + \phi_{zz} = 0 \quad \text{in } 0 < z < 1 + \alpha\eta, \quad (10)$$

$$\phi_z = 0 \quad \text{on } z = 0, \quad (11)$$

$$\eta_t + \alpha\phi_x\eta_x - \frac{1}{\beta}\phi_z = 0 \quad \text{on } z = 1 + \alpha\eta, \quad (12)$$

$$\beta\phi'_{xx} + \phi'_{zz} = 0 \quad \text{in } 1 + \alpha\eta < z < 1 + H, \quad (13)$$

$$\phi'_z = 0 \quad \text{on } z = 1 + H, \quad (14)$$

$$\eta_t + \alpha\phi'_x\eta_x - \frac{1}{\beta}\phi'_z = 0 \quad \text{on } z = 1 + \alpha\eta, \quad (15)$$

$$\left(\eta + \phi_t + \frac{1}{2}\alpha\phi_x^2 + \frac{1}{2}\frac{\alpha}{\beta}\phi_z^2 \right) = r \left(\eta + \phi'_t + \frac{1}{2}\alpha\phi'^2_x + \frac{1}{2}\frac{\alpha}{\beta}\phi'^2_z \right) \quad \text{on } z = 1 + \alpha\eta. \quad (16)$$

We represent the potential ϕ as a formal expansion,

$$\phi((x, z), t) = \sum_{m=0}^{\infty} f_m(x, t) z^m.$$

Demanding that ϕ formally satisfy Laplace's equation (10) leads to the recurrence relation

$$(m+2)(m+1)f_{m+2}(x, t) = -\beta(f_m(x, t))_{xx}, \quad \forall m = 0, 1, 2, \dots \quad (17)$$

Let $F(x, t) = f_0(x, t)$ denote the velocity potential at the bottom $z = 0$ and use (17) repeatedly to obtain

$$f_{2k}(x, t) = \frac{(-1)^k \beta^k}{(2k)!} \frac{\partial^{2k} F(x, t)}{\partial x^{2k}}, \quad \forall k = 0, 1, 2, \dots,$$

$$f_{2k+1}(x, t) = \frac{(-1)^k \beta^k}{(2k+1)!} \frac{\partial^{2k} f_1(x, t)}{\partial x^{2k}}, \quad \forall k = 0, 1, 2, \dots$$

Equation (11) implies that $f_1(x, t) = 0$, so

$$f_{2k+1}(x, t) = 0, \quad \forall k = 0, 1, 2, \dots, \quad (18)$$

and therefore

$$\phi((x, z), t) = \sum_{k=0}^{\infty} \frac{(-1)^k \beta^k}{(2k)!} \frac{\partial^{2k} F(x, t)}{\partial x^{2k}} z^{2k}.$$

Let $\partial F(x, t)/\partial x = u(x, t)$. Substitute the latter representation into (12) to obtain

$$\eta_t + u_x + \alpha(u\eta)_x - \frac{1}{6}\beta u_{xxx} - \frac{1}{2}\alpha\beta(\eta u_{xx})_x + \frac{1}{120}\beta^2 u_{xxxx} + O(\beta^3) = 0. \quad (19)$$

Similarly we represent the potential ϕ' as a formal expansion,

$$\phi'((x, z), t) = \sum_{m=0}^{\infty} f'_m(x, t)(1 + H - z)^m.$$

Demanding that ϕ' formally satisfy Laplace's equation (13) leads to the recurrence relation

$$(m+2)(m+1)f'_{m+2}(x, t) = -\beta(f'_m(x, t))_{xx}, \quad \forall m = 0, 1, 2, \dots \quad (20)$$

Let $F'(x, t) = f'_0(x, t)$ denote the velocity potential on the roof $z = 1 + H$ and use (20) repeatedly to obtain

$$\begin{aligned} f'_{2k}(x, t) &= \frac{(-1)^k \beta^k}{(2k)!} \frac{\partial^{2k} F'(x, t)}{\partial x^{2k}}, \quad \forall k = 0, 1, 2, \dots, \\ f'_{2k+1}(x, t) &= \frac{(-1)^k \beta^k}{(2k+1)!} \frac{\partial^{2k} f'_1(x, t)}{\partial x^{2k}}, \quad \forall k = 0, 1, 2, \dots \end{aligned}$$

Equation (14) implies that $f'_1(x, t) = 0$, so

$$f'_{2k+1}(x, t) = 0, \quad \forall k = 0, 1, 2, \dots, \quad (21)$$

and therefore

$$\phi'((x, z), t) = \sum_{k=0}^{\infty} \frac{(-1)^k \beta^k}{(2k)!} \frac{\partial^{2k} F'(x, t)}{\partial x^{2k}} (1 + H - z)^{2k}.$$

Let $\partial F'(x, t)/\partial x = u'(x, t)$. Substitute the latter representation into (15) to obtain

$$\begin{aligned} \eta_t - H u'_x + \alpha(u'\eta)_x + \frac{1}{6}\beta H^3 u'_{xxx} - \frac{1}{2}\alpha\beta H^2(\eta u'_{xx})_x \\ - \frac{1}{120}\beta^2 H^5 u'_{xxxxx} + O(\beta^3) = 0. \end{aligned} \quad (22)$$

It is important at this stage that $H = O(1)$.

Substitute the representations for ϕ and ϕ' into the dynamic condition (16) to obtain the third equation

$$\begin{aligned} (1-r)\eta + F_t - rF'_t - \frac{1}{2}\beta(u_{xt} - rH^2 u'_{xt}) \\ - \alpha\beta\eta(u_{xt} + rH u'_{xt}) + \frac{1}{24}\beta^2(u_{xxxt} - rH^4 u'_{xxxt}) \end{aligned}$$

$$+\frac{1}{2}\alpha(u^2 - \beta uu_{xx}) - \frac{1}{2}\alpha r(u'^2 - \beta H^2 u' u'_{xx}) + \frac{1}{2}\alpha\beta(u_x^2 - rH^2 u_x'^2) + O(\beta^3) = 0.$$

Differentiating with respect to x yields

$$\begin{aligned} (1-r)\eta_x + u_t - ru'_t - \frac{1}{2}\beta(u_{xxt} - rH^2 u'_{xxt}) + \alpha(uu_x - ru'u'_x) \\ - \alpha\beta(\eta u_{xt})_x - \alpha\beta rH(\eta u'_{xt})_x + \frac{1}{24}\beta^2(u_{xxxxt} - rH^4 u'_{xxxxt}) \\ - \frac{1}{2}\alpha\beta(uu_{xx} - rH^2 u' u'_{xx})_x + \alpha\beta(u_x u_{xx} - rH^2 u'_x u'_{xx}) + O(\beta^3) = 0. \end{aligned} \quad (23)$$

The three equations (19), (22) and (23) provide a Boussinesq system of equations describing waves at the interface $\eta(x, t)$ between two fluid layers based on the horizontal velocities u and u' along the bottom and the roof, respectively. It is correct up to second order in α, β .

One can derive a class of systems which are formally equivalent to the system we just derived. This will be accomplished by considering changes in the dependent variables and by making use of lower-order relations in higher-order terms. Toward this goal, begin by letting $w(x, t)$ be the scaled horizontal velocity corresponding to the physical depth $(1 - \theta)h$ below the unperturbed interface, and $w'(x, t)$ be the scaled horizontal velocity corresponding to the physical depth $(H - \theta')h$ above the unperturbed interface. The ranges for the parameters θ and θ' are $0 \leq \theta \leq 1$ and $0 \leq \theta' \leq H$. Note that $(\theta, \theta') = (0, 0)$ leads to $w = u$ and $w' = u'$, while $(\theta, \theta') = (1, H)$ leads to both velocities evaluated along the interface. A formal use of Taylor's formula with remainder shows that

$$\begin{aligned} w = \phi_x|_{z=\theta} &= \left(F_x - \frac{1}{2}\beta F_{xxx}\theta^2 + \frac{1}{24}\beta^2\theta^4 F_{xxxx} \right) + O(\beta^3) \\ &= u - \frac{1}{2}\beta\theta^2 u_{xx} + \frac{1}{24}\beta^2\theta^4 u_{xxxx} + O(\beta^3) \end{aligned}$$

as $\beta \rightarrow 0$. In Fourier space, the latter relationship may be written as

$$\hat{w} = \left(1 + \frac{1}{2}\beta\theta^2 k^2 + \frac{1}{24}\beta^2\theta^4 k^4 \right) \hat{u} + O(\beta^3).$$

Inverting the positive Fourier multiplier yields

$$\begin{aligned} \hat{u} &= \left(1 + \frac{1}{2}\beta\theta^2 k^2 + \frac{1}{24}\beta^2\theta^4 k^4 \right)^{-1} \hat{w} + O(\beta^3) \\ &= \left(1 - \frac{1}{2}\beta\theta^2 k^2 + \frac{5}{24}\beta^2\theta^4 k^4 \right) \hat{w} + O(\beta^3) \end{aligned}$$

as $\beta \rightarrow 0$. Thus there appears the relationship

$$u = w + \frac{1}{2}\beta\theta^2 w_{xx} + \frac{5}{24}\beta^2\theta^4 w_{xxxx} + O(\beta^3). \quad (24)$$

Similarly

$$\begin{aligned} w' &= \phi'_x|_{z=1+H-\theta'} = \left(F'_x - \frac{1}{2}\beta F'_{xxx}\theta'^2 + \frac{1}{24}\beta^2 F'_{xxxx}\theta'^4 \right) + O(\beta^3) \\ &= u' - \frac{1}{2}\beta\theta'^2 u'_{xx} + \frac{1}{24}\beta^2\theta'^4 u'_{xxxx} + O(\beta^3) \end{aligned}$$

and

$$\hat{w}' = \left(1 + \frac{1}{2}\beta\theta'^2 k^2 + \frac{1}{24}\beta^2\theta'^4 k^4 \right) \hat{u}' + O(\beta^3).$$

Inverting the positive Fourier multiplier yields

$$\hat{u}' = \left(1 - \frac{1}{2}\beta\theta'^2 k^2 + \frac{5}{24}\beta^2\theta'^4 k^4 \right) \hat{w}' + O(\beta^3)$$

and thus the relationship

$$u' = w' + \frac{1}{2}\beta\theta'^2 w'_{xx} + \frac{5}{24}\beta^2\theta'^4 w'_{xxxx} + O(\beta^3). \quad (25)$$

Substitute the expressions (24) and (25) for u and u' into (19) and (22), respectively, to obtain

$$\begin{aligned} &\eta_t + w_x + \alpha(w\eta)_x + \frac{1}{2}\beta \left(\theta^2 - \frac{1}{3} \right) w_{xxx} \\ &+ \frac{1}{2}\alpha\beta(\theta^2 - 1)(\eta w_{xx})_x + \frac{5}{24}\beta^2 \left(\theta^2 - \frac{1}{5} \right)^2 w_{xxxx} + O(\beta^3) = 0 \end{aligned} \quad (26)$$

$$\begin{aligned} &\eta_t - Hw'_x + \alpha(w'\eta)_x - \frac{1}{2}\beta H \left(\theta'^2 - \frac{1}{3}H^2 \right) w'_{xxx} \\ &+ \frac{1}{2}\alpha\beta \left(\theta'^2 - H^2 \right) (\eta w'_{xx})_x - \frac{5}{24}\beta^2 H \left(\theta'^2 - \frac{1}{5}H^2 \right)^2 w'_{xxxx} + O(\beta^3) = 0. \end{aligned} \quad (27)$$

Substitute the expressions (24) and (25) for u and u' into (23) to obtain

$$\begin{aligned} &(1-r)\eta_x + w_t - rw'_t + \frac{1}{2}\beta \left[(\theta^2 - 1)w - r(\theta'^2 - H^2)w' \right]_{xxt} + \alpha(w w_x - r w' w'_x) \\ &+ \frac{1}{24}\beta^2 \left[(\theta^2 - 1)(5\theta^2 - 1)w_{xxxxt} - r(\theta'^2 - H^2)(5\theta'^2 - H^2)w'_{xxxxt} \right] \end{aligned}$$

$$\begin{aligned}
& -\alpha\beta [(\eta w_{xt})_x + rH(\eta w'_{xt})_x] + \frac{1}{2}\alpha\beta [(\theta^2 - 1)ww_{xxx} - r(\theta'^2 - H^2)w'w'_{xxx}] \\
& + \frac{1}{2}\alpha\beta [(\theta^2 + 1)w_xw_{xx} - r(\theta'^2 + H^2)w'_xw'_{xx}] + O(\beta^3) = 0.
\end{aligned} \tag{28}$$

The system of three equations (26)–(28) is formally equivalent to the previous system but it allows one to choose the fluid levels θ and θ' as reference for the horizontal velocities. Among all these systems that model the same physical problem one can select those with the best dispersion relations. Neglecting terms of $O(\alpha^2, \beta^2, \alpha\beta)$, the system (26)–(28) reduces to

$$\begin{aligned}
& \eta_t + w_x + \alpha(w\eta)_x + \frac{1}{2}\beta(\theta^2 - \frac{1}{3})w_{xxx} = 0 \\
& \eta_t - Hw'_x + \alpha(w'\eta)_x - \frac{1}{2}\beta H(\theta'^2 - \frac{1}{3}H^2)w'_{xxx} = 0 \tag{29} \\
& (1-r)\eta_x + w_t - rw'_t + \frac{1}{2}\beta[(\theta^2 - 1)w - r(\theta'^2 - H^2)w']_{xxt} + \alpha(ww_x - rw'w'_x) = 0
\end{aligned}$$

4 System of two equations

The systems obtained in the previous section are not appropriate for numerical computations. One would like to obtain a system of two evolution equations for the variables η and $W = w - rw'$. In fact, Benjamin and Bridges [3] (see also [12,11,1]) formulated the interfacial wave problem using Hamiltonian formalism and showed that the canonical variables for interfacial waves are $\eta^*(x^*, t^*)$ and $\rho\phi^*(x^*, \eta^*, t^*) - \rho'\phi^{*'}(x^*, \eta^*, t^*)$.

At leading order, the first two equations of system (29) give

$$\begin{cases} \eta_t + w_x = 0, \\ \eta_t - Hw'_x = 0. \end{cases}$$

Assuming the fluids to be at rest as $x \rightarrow \infty$, one has $w = -Hw'$. Therefore

$$w = \frac{H}{r+H}W + O(\beta), \quad w' = \frac{-1}{r+H}W + O(\beta). \tag{30}$$

Adding H times the first equation to r times the second equation of system (29) yields

$$\begin{aligned}
& (r+H)\eta_t + H(w - rw')_x + \alpha[(Hw + rw')\eta]_x \\
& + \frac{H}{2}\beta[(\theta^2 - \frac{1}{3})w_{xxx} - r(\theta'^2 - \frac{1}{3}H^2)w'_{xxx}] = 0.
\end{aligned} \tag{31}$$

Using (30) and neglecting higher-order terms, one obtains

$$\eta_t = -\frac{H}{r+H}W_x - \alpha \frac{H^2-r}{(r+H)^2}(W\eta)_x - \beta \left(\frac{1}{2} \frac{H^2 S}{(r+H)^2} + \frac{1}{3} \frac{H^2(1+rH)}{(r+H)^2} \right) W_{xxx},$$

where

$$S = (\theta^2 - 1) + \frac{r}{H} (\theta'^2 - H^2).$$

In the third equation of system (29), the term with the txt -derivatives can be written as

$$\frac{1}{2}\beta \left[(\theta^2 - 1)w_{txt} - r(\theta'^2 - H^2)w'_{xt} \right] = \frac{1}{2}\beta \frac{HS}{r+H}W_{txt}.$$

The quadratic terms of the third equation of system (29) can be written as

$$\alpha(w w_x - r w' w'_x) = \alpha \frac{H^2 - r}{(r+H)^2} W W_x.$$

Then the third equation of system (29) becomes

$$W_t = -(1-r)\eta_x - \frac{1}{2}\beta \frac{HS}{r+H}W_{txt} - \alpha \frac{H^2 - r}{(r+H)^2} W W_x.$$

The final system of two equations for interfacial waves in the limit of long, weakly dispersive waves, can be written in terms of the horizontal velocities at arbitrary fluid levels as (in dimensionless form)

$$\begin{cases} \eta_t = -\frac{H}{r+H}W_x - \alpha \frac{H^2-r}{(r+H)^2}(W\eta)_x - \beta \left(\frac{1}{2} \frac{H^2 S}{(r+H)^2} + \frac{1}{3} \frac{H^2(1+rH)}{(r+H)^2} \right) W_{xxx} \\ W_t = -(1-r)\eta_x - \alpha \frac{H^2-r}{(r+H)^2} W W_x - \frac{1}{2}\beta \frac{HS}{r+H}W_{txt}, \end{cases} \quad (32)$$

or as (in physical variables)

$$\begin{cases} \eta_{t^*}^* = -h d_1 W_{x^*}^* - d_4 (W^* \eta^*)_{x^*} - h^3 d_2 W_{x^* x^* x^*}^*, \\ W_{t^*}^* = -g(1-r)\eta_{x^*}^* - d_4 W^* W_{x^*}^* - h^2 d_3 W_{x^* x^* t^*}^*, \end{cases} \quad (33)$$

where

$$d_1 = \frac{H}{r+H}, \quad d_2 = \frac{H^2}{2(r+H)^2} \left(S + \frac{2}{3}(1+rH) \right), \quad d_3 = \frac{1}{2} S d_1, \quad d_4 = \frac{H^2 - r}{(r+H)^2}. \quad (34)$$

Notice that Choi & Camassa [9] also derived a system of two equations (see their equations (3.33) and (3.34)), but it is different from ours. In particular, their coefficient d_2 is equal to 0, and their equation for W_t possesses an extra

quadratic term $\eta\eta_x$. The reason is that their ‘ W ’ is the mean horizontal velocity through the upper layer. The value of S which best approximates the Choi & Camassa equations is $S = -\frac{2}{3}(1 + rH)$. Indeed the coefficient d_2 then vanishes. This particular value for S can be explained as follows. The leading order correction to the horizontal velocity is given by

$$w(z) = u - \frac{1}{2}\beta z^2 u_{xx}.$$

The value of z , say $z = \theta$, for which the mean velocity

$$\bar{w} = \int_0^1 w(z) dz$$

is equal to $w(\theta)$ is given by $\theta = 1/\sqrt{3}$. Similarly, one finds $\theta' = (1/\sqrt{3})H$ for the upper layer. Therefore $S = -\frac{2}{3}(1 + rH)$.

Recall that the scaling that led to our Boussinesq system is given by

$$\frac{x^*}{h} = \frac{x}{\sqrt{\beta}}, \quad \frac{t^*}{h/c_0} = \frac{t}{\sqrt{\beta}}, \quad \frac{\eta^*}{h} = \alpha\eta, \quad \frac{W^*}{gh/c_0} = \alpha W,$$

with $c_0 = \sqrt{gh}$, $\alpha \ll 1$, $\beta \ll 1$ and $\alpha = O(\beta)$. Linearizing system (33) and looking for solutions (η^*, W^*) proportional to $\exp(ikx^* - i\omega t^*)$ leads to the dispersion relation

$$\frac{\omega^2}{k^2} = \frac{gh(1-r)(d_1 - d_2 k^2 h^2)}{1 - d_3 k^2 h^2}.$$

Plots of the dispersion relation are given in the next section. Since $0 \leq \theta \leq 1$ and $0 \leq \theta' \leq H$, the definition of S implies that

$$-1 - rH \leq S \leq 0.$$

It follows that $d_3 \leq 0$ and therefore the denominator $1 - d_3 h^2 k^2$ is positive. In order to have well-posedness (that is ω^2/k^2 positive for all values of k), d_2 must be negative, which is the case if $S \leq -\frac{2}{3}(1 + rH)$. Finally the condition we want to impose on S is that

$$-(1 + rH) \leq S \leq -\frac{2}{3}(1 + rH). \tag{35}$$

It is satisfied if one takes the horizontal velocities on the bottom and on the roof ($S = -(1 + rH)$) or the mean horizontal velocities in the bottom and upper layers ($S = -\frac{2}{3}(1 + rH)$), but it is not if one takes the horizontal velocities along the interface ($S = 0$).

5 The numerical scheme and numerical solutions

In order to integrate numerically the Boussinesq system (33), we introduce a slightly different change of variables, where the stars still denote the physical variables and no new notation is introduced for the dimensionless variables:

$$x = \frac{x^*}{h}, \quad \eta = \frac{\eta^*}{h}, \quad t = \frac{c}{h}t^*, \quad W = \frac{W^*}{c}, \quad \text{with } c^2 = gh \frac{H(1-r)}{r+H}.$$

The system (33) becomes

$$\begin{cases} \eta_t = -d_1 W_x - d_4 (W\eta)_x - d_2 W_{xxx} \\ W_t = -\frac{1}{d_1} \eta_x - d_4 W W_x - d_3 W_{xxt} \end{cases}, \quad (36)$$

with dispersion relation

$$\frac{\omega^2}{k^2} = \frac{d_1 - d_2 k^2}{d_1(1 - d_3 k^2)}. \quad (37)$$

As $k \rightarrow 0$, $\omega/k \rightarrow 1$. As $k \rightarrow \infty$,

$$\frac{\omega^2}{k^2} \rightarrow \frac{d_2}{d_1 d_3} = 1 + \frac{2(1+rH)}{3S}.$$

Typical plots of the dispersion relation (37) are given in Figure 2. Comparisons between the approximate and the exact dispersion relations, given by

$$\frac{\omega^2}{k^2} = \frac{\tanh k \tanh kH}{d_1 k (\tanh kH + r \tanh k)}$$

are also shown. A very good agreement is found for small k . Taking the Fourier transform of the system (36) gives

$$\begin{cases} \hat{\eta}_t = (d_2 k^2 - d_1) i k \hat{W} - d_4 i k \widehat{W\eta} \\ \hat{W}_t = -\frac{1}{d_1(1 - d_3 k^2)} i k \hat{\eta} - \frac{d_4}{2(1 - d_3 k^2)} i k \widehat{W^2} \end{cases}.$$

The system of differential equations is solved by a pseudo-spectral method in space with a number N of Fourier modes on a periodic domain of length L . For most applications, $N = 1024$ was found to be sufficient. The time integration is performed using the classical fourth-order explicit Runge–Kutta scheme. The time step Δt was optimized through a trial and error process and was found to have a dependence in $1/N$.

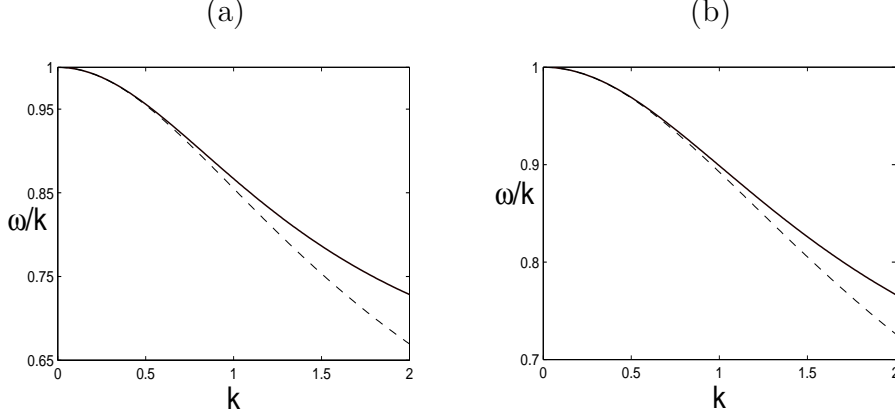


Fig. 2. Dispersion relation (37) for the Boussinesq system (36) with $S = -1 - rH$, $r = 0.9$: (a) $H = 1.2$, (b) $H = 0.8$. The dashed curves represent the dispersion relation for the linearized interfacial wave equations, without the long wave assumption (see for example [22]).

Since the main goal is to study the propagation and the collision of solitary waves, we first look for solitary wave solutions of the system (36). As opposed to the KdV equation, there are no explicit solitary wave solutions of the Boussinesq system that are physically relevant. Therefore we look for an approximate solitary wave solution to (36) as in [4] (see also [15] for the existence of solitary wave solutions). The leading-order terms give

$$\eta_t = -d_1 W_x, \quad W_t = -\frac{1}{d_1} \eta_x.$$

A solution representing a right-running wave is

$$W(x - t) = \frac{1}{d_1} \eta(x - t).$$

Let us look for solutions of system (36) in the form

$$W(x, t) = \frac{1}{d_1} [\eta(x, t) + M(x, t)],$$

where M is assumed to be small compared to η and W . Substituting the expression for W into (36) and neglecting higher-order terms yields

$$\begin{cases} \eta_t = -\eta_x - M_x - \frac{d_4}{d_1} (\eta^2)_x - \frac{d_2}{d_1} \eta_{xxx} \\ \eta_t = -\eta_x - M_t - \frac{1}{2} \frac{d_4}{d_1} (\eta^2)_x - d_3 \eta_{xxt} \end{cases}. \quad (38)$$

Assuming that the solitary wave goes to the right, one has $M_t \approx -M_x$. Therefore

$$M_x = -\frac{1}{4} \frac{d_4}{d_1} (\eta^2)_x - \frac{1}{2} \frac{d_2}{d_1} \eta_{xxx} + \frac{1}{2} d_3 \eta_{xxt}.$$

Substituting the expression for M_x into one of the equations of system (38) yields

$$\eta_t + \eta_x + \frac{3d_4}{4d_1} (\eta^2)_x + \frac{d_2}{2d_1} \eta_{xxx} + \frac{d_3}{2} \eta_{xxt} = 0. \quad (39)$$

This is essentially the model equation that was studied in [7].

Looking for solitary wave solutions of (39) in the form

$$\eta = \eta_0 \operatorname{sech}^2[\kappa(x + x_0 - Vt)] \quad (40)$$

leads to two equations for κ and V :

$$\begin{cases} -V + 1 + 2(d_2/d_1)\kappa^2 - 2d_3\kappa^2V = 0 \\ d_4\eta_0 - 4d_2\kappa^2 + 4d_1d_3\kappa^2V = 0 \end{cases}.$$

Solving for κ^2 and V yields

$$\kappa^2 = \frac{d_4\eta_0}{4\left(d_2 - d_1d_3 - \frac{1}{2}d_3d_4\eta_0\right)}, \quad V = 1 + \frac{d_4\eta_0}{2d_1},$$

and, assuming $M(\pm\infty) = 0$, one obtains explicitly the following expression for M :

$$M = -\frac{d_4}{4d_1} \eta^2 - \frac{d_2}{2d_1} \eta_{xx} + \frac{d_3}{2} \eta_{xt}.$$

For a given pair (r, H) , one must only consider values of η_0 which are such that $\kappa^2 > 0$. In addition one has the condition (35) on S . The sign of d_4 depends on the relation between H^2 and r . Let us assume first that $H^2 > r$ so that $d_4 > 0$. In order for the condition $\kappa^2 > 0$ to be satisfied, one needs

$$\eta_0 \left(d_2 - d_1d_3 - \frac{1}{2}d_3d_4\eta_0 \right) > 0.$$

The values of η_0 for which the left-hand side of the inequality vanishes are

$$\eta_{01} = 0, \quad \eta_{02} = \frac{4H(r+H)(1+rH)}{3(H^2-r)S}.$$

Since $S < 0$, $\eta_{02} < 0$ and therefore $\eta_{02} < \eta_{01}$. The coefficient of η_0^2 in the inequality is positive. Consequently one must have

$$\eta_0 > \eta_{01} = 0 \quad \text{or} \quad \eta_0 < \eta_{02} = \frac{4H(r+H)(1+rH)}{3(H^2-r)S}.$$

This second branch is not acceptable since

$$\frac{4H(r+H)(1+rH)}{3(H^2-r)} > 1+rH > -S > 0.$$

Therefore

$$\frac{4H(r+H)(1+rH)}{3(H^2-r)S} < -1,$$

which gives an amplitude larger than the depth!

Similarly, when $H^2 < r$ one finds a second branch which is not acceptable. The summary of acceptable values for η_0 is given in the table

$H^2 - r > 0$	$0 < \eta_0 < H$
$H^2 - r < 0$	$-1 < \eta_0 < 0$

For a “thick” upper layer ($H^2 > r$), the solitary waves are of elevation, while they are of depression for a “thick” bottom layer ($H^2 < r$). The weakly nonlinear theory developed in the present section does not provide any bounds on the amplitude of the solitary waves. We have added a physical constraint based on the fact that both layers are bounded by flat solid boundaries. It is well-known in the framework of the full interfacial wave equations (see for example [22]) that the rigid top and bottom provide natural bounds on the solitary wave amplitudes. As the speed increases, the wave amplitude reaches a limit. In the next section, we extend our weakly nonlinear analysis to cubic terms so that this effect can be incorporated.

Once the approximate solitary wave (40) has been obtained, it is possible to make it cleaner by iterative filtering. This technique has been used by several authors, including [4,6], and is explained in Appendix A. In order to study run-ups and phase shifts during collision of solitary waves, it is important to use clean solitary waves for the initial conditions. On the other hand, in order to show only the qualitative behavior, it is not necessary. Therefore results in this Section are given for non-filtered solitary waves. Some results with filtered waves are described in Appendix A.

In Figure 3, we show the propagation of an almost perfect right-running solitary wave of elevation. Even though all computations are performed with dimensionless variables, it is interesting to provide numerical applications for a configuration that could be realized in the laboratory [23]. Keeping $r = 0.9$

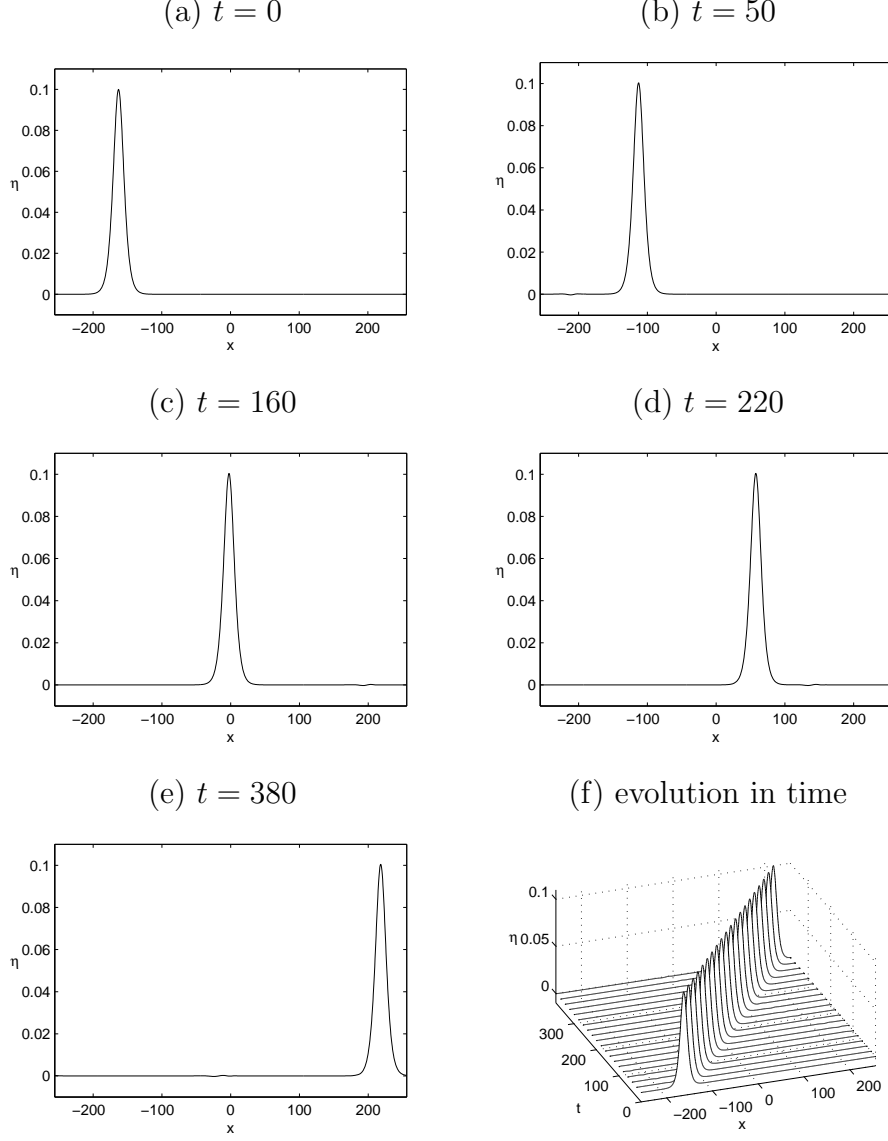


Fig. 3. An approximate solitary wave propagating to the right. This is a solution to the system of quadratic Boussinesq equations (36), with parameters $H = 1.1$, $r = 0.9$, $L = 512$, $N = 1024$, $S = -1 - rH$, $\eta_0 = 0.1$.

as in the figure, one could take for example $h = 10$ cm, $h' = 11$ cm ($H = 1.1$). The solitary wave amplitude is 1 cm, its speed $c \approx 23.2$ cm/s, the length of the domain 51.2 m (a bit long!). The plots (b)–(e) would then correspond to snapshots at $t = 21.5$ s, $t = 68.9$ s, $t = 94.8$ s and $t = 163.7$ s.

In Figure 4, we show the head-on collision of two almost perfect solitary waves of elevation of equal amplitude moving in opposite directions. As in the one-layer case, the solution rises to an amplitude slightly larger than the sum of the amplitudes of the two incident solitary waves (see Appendix A). After the collision, two similar waves emerge and return to the form of two separated solitary waves. As a result of this collision, the amplitudes of the two result-

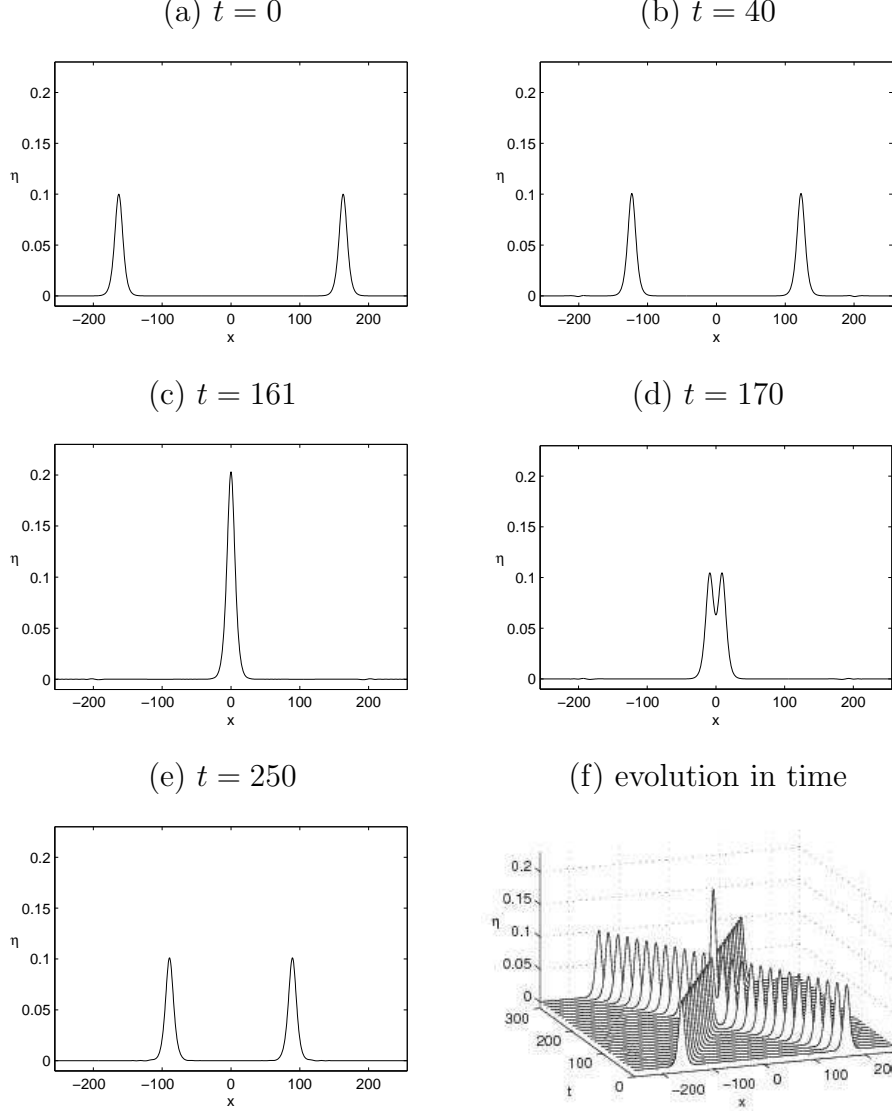


Fig. 4. Head-on collision of two approximate solitary waves of elevation of equal size. This is a solution to the system of quadratic Boussinesq equations (36), with parameters $H = 1.2$, $r = 0.8$, $L = 512$, $N = 1024$, $S = -1 - rH$, $\eta_0^\ell = \eta_0^r = 0.1$, where the superscripts ℓ and r stand for left and right respectively.

ing solitary waves are slightly smaller than the incident amplitudes and their centers are slightly retarded from the trajectories of the incoming centers (see again Appendix A).

In Figure 5, we show the collision of two almost perfect solitary waves of depression of unequal amplitudes moving in opposite directions. The numerical simulations exhibit a number of the same features that have been observed in the symmetric case.

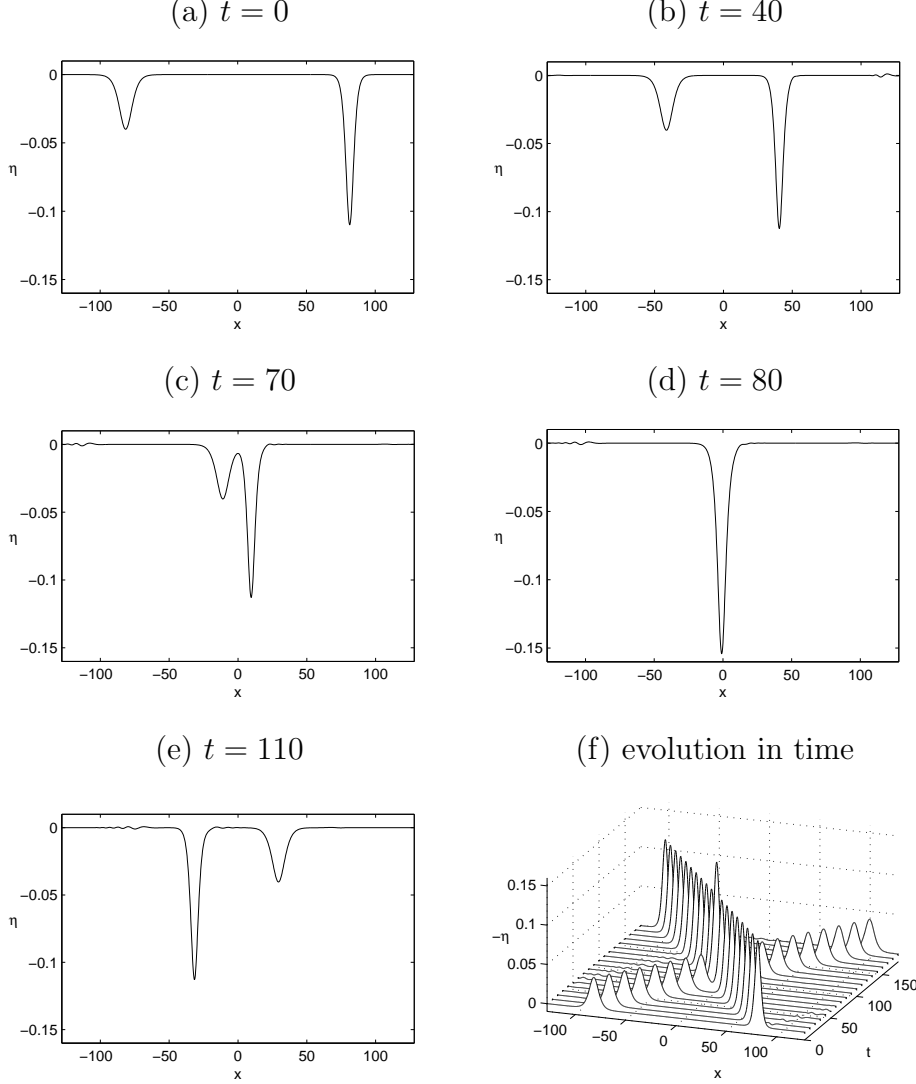


Fig. 5. Head-on collision of two almost perfect solitary waves of depression of different sizes. This is a solution to the system of quadratic Boussinesq equations (36), with parameters $H = 0.6$, $r = 0.85$, $L = 256$, $N = 1024$, $S = -1 - rH$, $\eta_0^\ell = -0.04$, $\eta_0^r = -0.11$, where the superscripts ℓ and r stand for left and right respectively. In plot (f), note that $-\eta(x, t)$ has been plotted for the sake of clarity.

In Figure 6, we show the co-propagation of two solitary waves of elevation of different amplitudes. A sequence of spatial profiles is shown. The larger one, which is faster, eventually passes the smaller one, which is slower. Again there is a phase shift after the interaction. The amplitude of the solution $\eta(x, t)$ never exceeds that of the larger solitary wave, nor does it dip below the amplitude of the smaller.

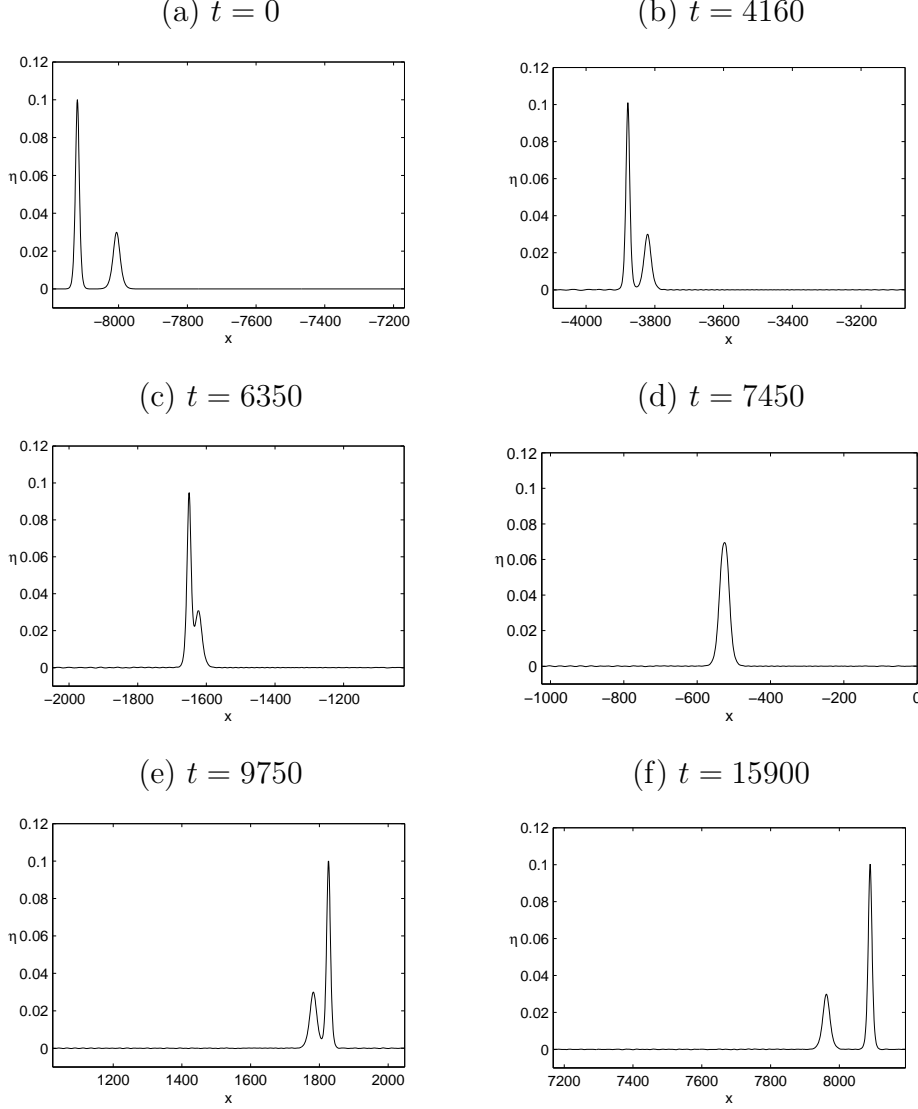


Fig. 6. Co-propagation of two almost perfect solitary waves of elevation of different sizes. This is a solution to the system of quadratic Boussinesq equations (36), with parameters $H = 1.6$, $r = 0.95$, $L = 2^{14}$, $N = 2^{14}$, $S = -1 - rH$, $\eta_0^\ell = 0.1$, $\eta_0^r = 0.03$, where the superscripts ℓ and r stand for left and right respectively.

6 Extended Boussinesq system of two equations with cubic terms

When $|H^2 - r|$ is small, one needs to go one step beyond and take into consideration the cubic terms. Again one would like to obtain a system of two equations for the variables η and $W = w - rw'$. We derive first a general system of two equations with cubic terms. Then we introduce a specific scaling for the case where $|H^2 - r|$ is small. A lot of terms in the system drop out because they are of higher order.

The leading order terms lead to the same equation as before, namely $w = -Hw'$. And again

$$w = \frac{H}{r+H}W + O(\beta), \quad w' = \frac{-1}{r+H}W + O(\beta). \quad (41)$$

At the next order, the first two equations of (29) give

$$w_x + \alpha(w\eta)_x + \frac{1}{2}\beta\left(\theta^2 - \frac{1}{3}\right)w_{xxx} = -Hw'_x + \alpha(w'\eta)_x - \frac{1}{2}\beta H\left(\theta'^2 - \frac{1}{3}H^2\right)w'_{xx}.$$

Since the speeds w and w' vanish as $x \rightarrow \infty$ one has

$$w = -Hw' + \alpha(w' - w)\eta - \frac{1}{2}\beta\left(H\left(\theta'^2 - \frac{1}{3}H^2\right)w'_{xx} + \left(\theta^2 - \frac{1}{3}\right)w_{xx}\right).$$

Using (41) for the terms containing α or β and neglecting terms of $O(\beta^2)$, one obtains

$$w = -Hw' - \alpha\frac{1+H}{r+H}W\eta + \frac{1}{2}\beta H\frac{\left(\theta'^2 - \frac{1}{3}H^2\right) - \left(\theta^2 - \frac{1}{3}\right)}{r+H}W_{xx}, \quad (42)$$

$$w' = -\frac{w}{H} - \alpha\frac{1+H}{H(r+H)}W\eta + \frac{1}{2}\beta\frac{\left(\theta'^2 - \frac{1}{3}H^2\right) - \left(\theta^2 - \frac{1}{3}\right)}{r+H}W_{xx}. \quad (43)$$

In Appendix B, after several substitutions, one obtains the system of two equations (B.8) and (B.15). Switching back to the physical variables

$$x^* = \ell x, \quad \eta^* = A\eta, \quad t^* = \ell t/c_0, \quad W^* = gAW/c_0, \quad \text{with } c_0 = \sqrt{gh},$$

the system (B.8)-(B.15) becomes

$$\begin{aligned} & (r+H)\eta_{t^*}^* + hHW_{x^*}^* + \frac{H^2-r}{r+H}(W^*\eta^*)_{x^*} + \frac{1}{2}h^3H\frac{H(\theta'^2-\frac{1}{3})+r(\theta'^2-\frac{1}{3}H^2)}{r+H}W_{x^*x^*x^*}^* \\ & - \frac{1}{h}\frac{r(1+H)^2}{(r+H)^2}(W^*\eta^{*2})_{x^*} + \frac{1}{2}h^2rH(1+H)\frac{(\theta'^2-\frac{1}{3}H^2)-(\theta^2-\frac{1}{3})}{(r+H)^2}(W^*\eta^*)_{x^*x^*x^*} \\ & + \frac{1}{2}h^2\left(rH(1+H)\frac{(\theta'^2-\frac{1}{3}H^2)-(\theta^2-\frac{1}{3})}{(r+H)^2} + \frac{H^2(\theta^2-1)-r(\theta'^2-H^2)}{r+H}\right)(W_{x^*x^*}^*\eta^*)_{x^*} \\ & - \frac{1}{4}h^5\left(\frac{rH^2((\theta'^2-\frac{1}{3}H^2)-(\theta^2-\frac{1}{3}))^2}{(r+H)^2} - \frac{5}{6}\frac{H^2(\theta^2-\frac{1}{5})^2+rH(\theta'^2-\frac{1}{5}H^2)^2}{r+H}\right)W_{x^*x^*x^*x^*x^*}^* = 0, \end{aligned} \quad (44)$$

$$\begin{aligned}
& g(1-r)\eta_{x^*}^* + W_{t^*}^* + \frac{H^2-r}{(r+H)^2}W^*W_{x^*}^* + \frac{1}{2}h^2\frac{H(\theta^2-1)+r(\theta'^2-H^2)}{r+H}W_{x^*x^*t^*}^* \\
& - \frac{1}{h}\frac{r(1+H)^2}{(r+H)^3}(W^{*2}\eta^*)_{x^*} + \frac{1}{2}h^2rH(1+H)\frac{(\theta'^2-\frac{1}{3}H^2)-(\theta^2-\frac{1}{3})}{(r+H)^3}(W^*W_{x^*x^*}^*)_{x^*} \\
& + h\frac{H(1-r)}{r+H}(\eta^*W_{x^*t^*}^*)_{x^*} + \frac{1}{2}h^2\frac{H^2(\theta^2-1)-r(\theta'^2-H^2)}{(r+H)^2}W^*W_{x^*x^*x^*}^* \\
& + \frac{1}{2}h^2\frac{H^2(\theta^2+1)-r(\theta'^2+H^2)}{(r+H)^2}W_{x^*}^*W_{x^*x^*}^* - \frac{1}{2}hrH(1+H)\frac{(\theta^2-1)-(\theta'^2-H^2)}{(r+H)^2}(W^*\eta^*)_{x^*x^*t^*} \\
& + h^4\left(\frac{rH((\theta^2-1)-(\theta'^2-H^2))((\theta'^2-\frac{1}{3}H^2)-(\theta^2-\frac{1}{3}))}{4(r+H)^2} + \frac{H(\theta^2-1)(5\theta^2-1)+r(\theta'^2-H^2)(5\theta'^2-H^2)}{2(r+H)}\right) \\
& W_{x^*x^*x^*x^*t^*}^* = 0.
\end{aligned} \tag{45}$$

The specific scaling for small values of $|H^2 - r|$,

$$\frac{x^*}{h} = \frac{x}{\beta}, \quad \frac{t^*}{h/c_0} = \frac{t}{\alpha}, \quad \frac{\eta^*}{h} = \alpha\eta, \quad \frac{W^*}{gh/c_0} = \alpha W, \quad H^2 - r = \alpha\mathcal{C},$$

with $c_0 = \sqrt{gh}$, $\alpha \ll 1$, $\beta \ll 1$, $\alpha = O(\beta)$, will lead to a new Boussinesq system with cubic terms. A lot of terms in (44)-(45) drop out because they are of higher order. Keeping terms of order α^2 and α^4 and going back to physical variables, the system of two equations becomes

$$\begin{aligned}
\eta_{t^*}^* &= -h\frac{H}{r+H}W_{x^*}^* - h^3\left(\frac{1}{2}\frac{H^2S}{(r+H)^2} + \frac{1}{3}\frac{H^2(1+rH)}{(r+H)^2}\right)W_{x^*x^*x^*}^* \\
& - \frac{H^2-r}{(r+H)^2}(W^*\eta^*)_{x^*} + \frac{1}{h}\frac{r(1+H)^2}{(r+H)^3}(W^*\eta^{*2})_{x^*} \\
W_{t^*}^* &= -g(1-r)\eta_{x^*}^* - \frac{1}{2}h^2\frac{HS}{r+H}W_{x^*x^*t^*}^* - \frac{H^2-r}{(r+H)^2}W^*W_{x^*}^* + \frac{1}{h}\frac{r(1+H)^2}{(r+H)^3}(W^{*2}\eta^*)_{x^*}.
\end{aligned} \tag{46}$$

This is the same system as (33) with two extra terms, the cubic terms. We will call it a system of extended Boussinesq equations (see also [11]). Linearizing (46) gives the same dispersion relation as before.

7 Numerical solutions of the extended Boussinesq system

In order to integrate numerically the extended Boussinesq system (46), we introduce a slightly different change of variables, where the stars still denote the physical variables and no new notation is introduced for the dimensionless variables:

$$x = \frac{x^*}{h}, \quad \eta = \frac{\eta^*}{h}, \quad t = \frac{c}{h}t^*, \quad W = \frac{W^*}{c}, \quad \text{with } c^2 = \frac{ghh'(\rho - \rho')}{\rho'h + \rho h'} = \frac{ghH(1-r)}{r+H}.$$

Using the same coefficients as in (34), we rewrite system (46) with the new variables as

$$\begin{aligned}\eta_t &= -d_1 W_x - d_2 W_{xxx} - d_4 (W\eta)_x + d_5 (W\eta^2)_x \\ W_t &= -(1/d_1)\eta_x - d_3 W_{xxt} - d_4 W W_x + d_5 (W^2\eta)_x\end{aligned}\tag{47}$$

where the new coefficient d_5 is equal to

$$d_5 = \frac{r(1+H)^2}{(r+H)^3}.$$

When $(\theta, \theta') = (0, 0)$, one recovers the system with horizontal velocities on the bottom and on the roof.

Taking the Fourier transform of the system (47) gives

$$\begin{aligned}\hat{\eta}_t &= (d_2 k^2 - d_1)ik\hat{W} - d_4 ik\widehat{(W\eta)} + d_5 ik\widehat{(W\eta^2)}, \\ (1 - d_3 k^2)\hat{W}_t &= -\frac{1}{d_1}ik\hat{\eta} - \frac{d_4}{2}ik\widehat{(W^2)} + d_5 ik\widehat{(W^2\eta)}.\end{aligned}$$

The system of differential equations is integrated numerically with the same method as in § 5.

Again we look for approximate solitary wave solutions to (47). As before we look for solutions of the form

$$W(x, t) = \frac{1}{d_1}[\eta(x, t) + M(x, t)],$$

where M is assumed to be small compared to η and W . Substituting the expression for W into (47) and neglecting higher-order terms yields

$$M_x = -\frac{1}{4}\frac{d_4}{d_1}(\eta^2)_x - \frac{1}{2}\frac{d_2}{d_1}\eta_{xxx} + \frac{1}{2}d_3\eta_{xxt}.\tag{48}$$

Substituting the expression for M_x into one of the equations of system (47) yields

$$\eta_t + \eta_x + \frac{3d_4}{4d_1}(\eta^2)_x - \frac{d_5}{d_1}(\eta^3)_x + \frac{d_2}{2d_1}\eta_{xxx} + \frac{d_3}{2}\eta_{xxt} = 0.\tag{49}$$

We have checked that the extended KdV equation (49) is in agreement with previously derived eKdV equations such as in [14].

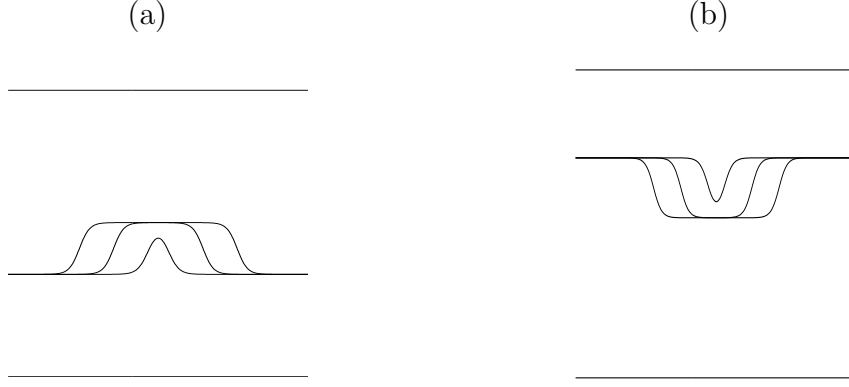


Fig. 7. ‘Table-top’ solitary waves which are approximate solutions of the extended Boussinesq system (47). The horizontal velocities are taken on the top and the bottom so that $S = -(1 + rH)$. (a) $H = 1.8$, $r = 0.8$. The wave speeds V are, going from the smallest to the widest solitary wave, $V_{\max} - V \sim 10^{-3}, 10^{-9}, 10^{-15}$; (b) $H = 0.4$, $r = 0.9$. The wave speeds V are, going from the smallest to the widest solitary wave, $V_{\max} - V \sim 10^{-3}, 10^{-9}, 10^{-14}$.

Let $V = 1 + c_1$ be the wave speed, with c_1 small. In the moving frame of reference $X = x - (1 + c_1)t$, $T = t$, equation (49) becomes

$$-c_1\eta_X + \eta_T + \frac{3d_4}{4d_1}(\eta^2)_X - \frac{d_5}{d_1}(\eta^3)_X + \frac{d_2}{2d_1}\eta_{XXX} + \frac{d_3}{2}[-(1 + c_1)\eta_{XXX} + \eta_{XXT}] = 0.$$

Looking for stationary solutions and integrating with respect to X yields

$$-c_1\eta + \frac{3d_4}{4d_1}\eta^2 - \frac{d_5}{d_1}\eta^3 + \frac{1}{2}\left(\frac{d_2}{d_1} - d_3 - c_1d_3\right)\eta_{XX} = 0. \quad (50)$$

Letting

$$\alpha_1 = \frac{3}{2} \frac{H^2 - r}{H(r + H)}, \quad \beta_1 = 3 \frac{r(1 + H)^2}{H(r + H)^2}, \quad \lambda_1 = \frac{1}{6} \frac{H(rH + 1)}{r + H} - \frac{1}{4} \frac{HS}{r + H} c_1,$$

equation (50) becomes

$$-c_1\eta + \frac{1}{2}\alpha_1\eta^2 - \frac{1}{3}\beta_1\eta^3 + \lambda_1\eta_{XX} = 0.$$

It has solitary wave solutions

$$\eta(X) = \left(\frac{\alpha_1}{\beta_1}\right) \frac{1 - \epsilon^2}{1 + \epsilon \cosh(\sqrt{\frac{c_1}{\lambda_1}} X)}, \quad \text{with } \epsilon = \frac{\sqrt{\alpha_1^2 - 6\beta_1 c_1}}{|\alpha_1|}.$$

In the fixed frame of reference, the profile of the solitary waves is given by

$$\eta(x, t) = \left(\frac{\alpha_1}{\beta_1} \right) \frac{1 - \epsilon^2}{1 + \epsilon \cosh \left(\sqrt{\frac{V-1}{\lambda_1}} (x - Vt) \right)}. \quad (51)$$

When $H^2 > r$ the solitary waves are of elevation. When $H^2 < r$ they are of depression. The parameter ϵ can take values ranging from 0 (infinitely wide solution) to 1 (solution of infinitesimal amplitude). Assuming $M(\pm\infty) = 0$, one can compute M explicitly by integrating equation (48) with respect to x :

$$M = -\frac{d_4}{4d_1}\eta^2 - \frac{d_2}{2d_1}\eta_{xx} + \frac{d_3}{2}\eta_{xt}.$$

Typical approximate solitary waves solutions are shown in Figure 7. Notice that the condition $|H^2 - r|$ small is not really satisfied for the selected values of H and r . The reason is that otherwise the waves would have been too small to be clearly visible. Of course we still have the conditions on S for well-posedness:

$$-(1 + rH) \leq S \leq -\frac{2}{3}(1 + rH).$$

The solitary waves are characterized by wave velocities larger than 1 ($c_1 > 0$). The maximum wave velocity V_{\max} is obtained when $\epsilon \rightarrow 0$. One finds $c_1 \rightarrow \alpha_1^2/6\beta_1$, so that

$$V_{\max} = 1 + \frac{(H^2 - r)^2}{8rH(1 + H)^2}.$$

Once the approximate solitary wave (51) has been obtained, it is again possible to make it cleaner by iterative filtering. Qualitative results for non-filtered solitary waves are given in this Section. Some accurate results for run-ups and phase shifts with filtered waves are described in Appendix A.

In Figure 8, we show the head-on collision of two almost perfect ‘table-top’ solitary waves of elevation of equal amplitude moving in opposite directions. As in the case with only quadratic nonlinearities, the solution rises to an amplitude larger than the sum of the amplitudes of the two incident solitary waves. After the collision, two similar waves emerge and return to the form of two separated ‘table-top’ solitary waves. As a result of this collision, the amplitudes of the two resulting solitary waves are slightly smaller than the incident amplitudes and their centers are slightly retarded from the trajectories of the incoming centers.

In Figure 9, we show the collision of two almost perfect solitary waves of depression of equal amplitude moving in opposite directions. The numerical simulations exhibit the same features that have been observed in the elevation case.

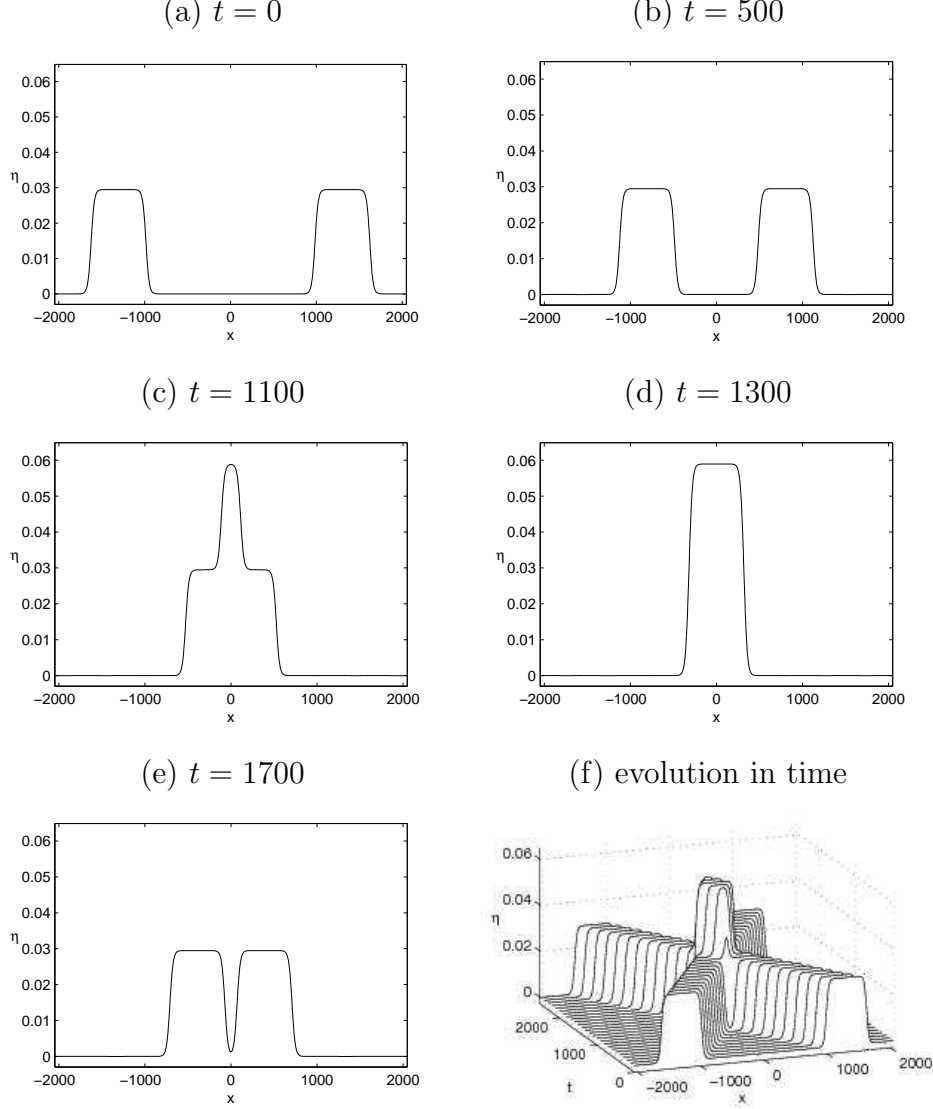


Fig. 8. Head-on collision of two approximate ‘table-top’ elevation solitary waves of equal size. This is a solution to the system of cubic Boussinesq equations (47), with parameters $H = 0.95$, $r = 0.8$, $L = 4096$, $N = 1024$, $S = -1 - rH$, $V_{\max} - V \sim 10^{-17}$.

In Figure 10, we show the collision of an almost perfect ‘table-top’ solitary wave of elevation with a solitary wave of elevation moving in the opposite direction. The numerical simulations exhibit a number of the same features that have been observed in the symmetric case. The phase lag is asymmetric, with the smaller solitary wave being delayed more significantly than the larger.

Note that in the quadratic as well as in the cubic cases, it is not possible to consider the collision between a solitary wave of depression and a solitary wave of elevation. Indeed the sign of $H^2 - r$ determines whether the wave is of elevation or of depression.

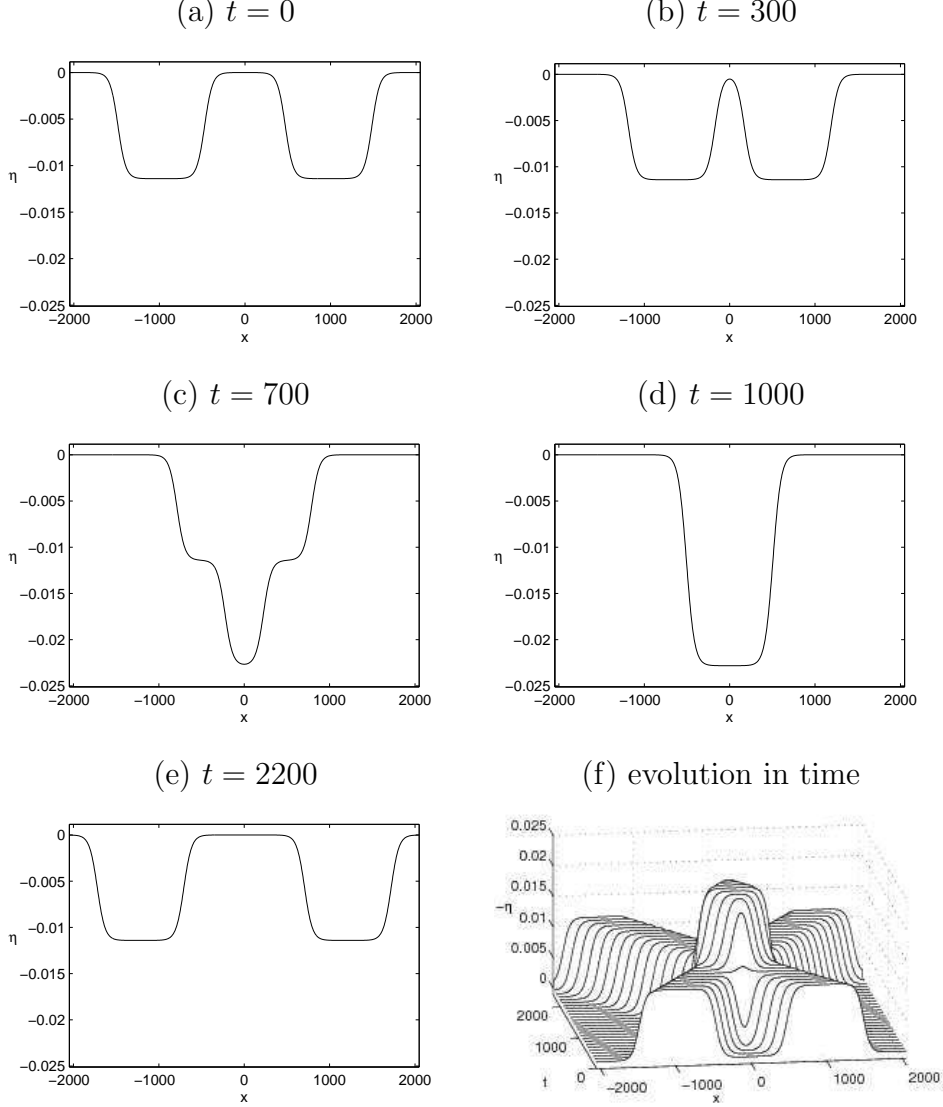


Fig. 9. Head-on collision of two approximate ‘table-top’ depression solitary waves of equal size. This is a solution to the system of cubic Boussinesq equations (47), with parameters $H = 0.9$, $r = 0.85$, $L = 4096$, $N = 1024$, $S = -1 - rH$, $V_{\max} - V \sim 10^{-14}$. In plot (f), note that $-\eta(x, t)$ has been plotted for the sake of clarity.

8 Conclusion

In this paper, we derived a system of extended Boussinesq equations in order to describe weakly nonlinear waves at the interface between two heavy fluids in a ‘rigid-lid’ configuration. To our knowledge we have described for the first time the collision between ‘table-top’ solitary waves. The extension to a ‘free-surface’ configuration and to arbitrary wave amplitude is left to future studies. Indeed, since the waves we considered are only weakly nonlinear, we do not have to worry about the resulting wave reaching the roof or the bottom.

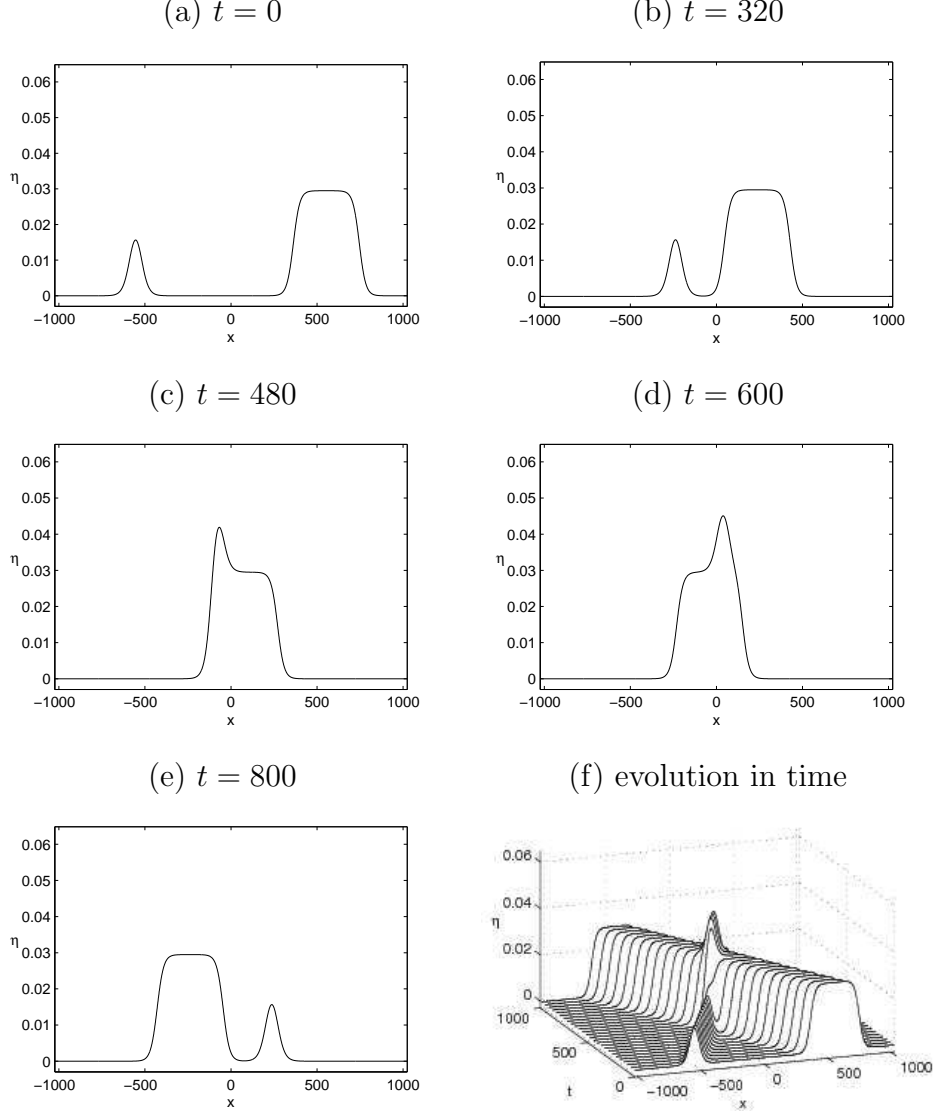


Fig. 10. Head-on collision of a solitary wave of elevation and of a ‘table-top’ solitary wave of elevation. This is a solution to the system of cubic Boussinesq equations (47), with parameters $H = 0.95$, $r = 0.8$, $L = 2048$, $N = 1024$, $S = -1 - rH$, $V_{\max} - V^\ell \sim 10^{-4}$, $V_{\max} - V^r \sim 10^{-11}$.

However, in a fully nonlinear regime, this could happen. Indeed the maximum amplitude A for ‘table-top’ solitary waves is given by

$$\frac{A}{h} = \frac{H - \sqrt{r}}{1 + \sqrt{r}}.$$

Take the case where $H^2 > r$. It is easy to see that while A/h is always smaller than H , $2A/h$ can exceed H , so that the resulting wave will hit the roof. Therefore it will be interesting to consider the collision of solitary waves of arbitrary amplitudes by using the full Euler equations. On the other hand, for ‘table-top’ solitary waves of depression, the resulting wave cannot touch the

bottom.

A Additional results on run-ups and phase shifts

In this appendix, we provide accurate results on run-ups and phase shifts. The terminology ‘run-up’ denotes the fact that during the collision of two counterpropagating solitary waves the wave amplitude increases beyond the sum of the two single wave amplitudes. Since run-ups and phase shifts are always very small, they must be computed with high accuracy. This is why it is important to clean the solitary waves obtained by the approximate expressions (40) or (51). We proceed as follows. We begin with an approximate solution, let it propagate across the domain, truncate the leading pulse, use it as new initial value by translating it to the left of the domain, let it propagate again and distance itself from the trailing dispersive tail, truncate again, and repeat the whole process over and over until a clean, at least to the eye, solitary wave is produced. Then we use this new filtered solution as initial guess to study the various collisions.

For solitary wave solutions to the system of equations with quadratic nonlinearities (36), the behavior is the same as the behavior shown for example in [10]. In particular we obtain pictures that look very similar to their Figure 2 for the phase shift resulting from the head-on collision of two solitary waves of equal height, to their Figure 4 for the time evolution of the maximum amplitude of the solution (it rises sharply to more than twice the elevation of the incident solitary waves, then descends to below this level after crest detachment, and finally relaxes back to almost its initial level) and to their Figure 12 for the asymmetric head-on collision of two solitary waves of different heights.

Since the main contribution of the present paper is the inclusion of cubic terms in addition to the quadratic terms, we focus on results for the extended Boussinesq system (46). Figure A.1 shows the effect of cleaning. In Figure A.2, the collision between two clean ‘table-top’ solitary waves (the cleaning has been applied 400 times) is shown. Their speed is $V = 1.00183358$. The amplitude before cleaning was $\eta_{\max} = 0.063476$. After iterative cleaning, it reached $\eta_{\max} = 0.06812113$. The run-up during collision is extremely small: indeed $\eta_{\max} = 0.13624323$ at collision, which is slightly larger than $2 \times 0.06812113 = 0.13624226$. The phase shift is also very small. In Figure A.3, the collision between the clean ‘table-top’ solitary wave of the Figure A.1 and a clean solitary wave (the cleaning has been applied 230 times) is shown. The maximum amplitude is greater than the sum of the two wave amplitudes. The speed of the smaller wave is $V = 1.0015$. Its amplitude before cleaning was $\eta_{\max} = 0.03647847$. After iterative cleaning, it reached $\eta_{\max} = 0.03719492$. The run-up during collision is again extremely small, even if it is larger than

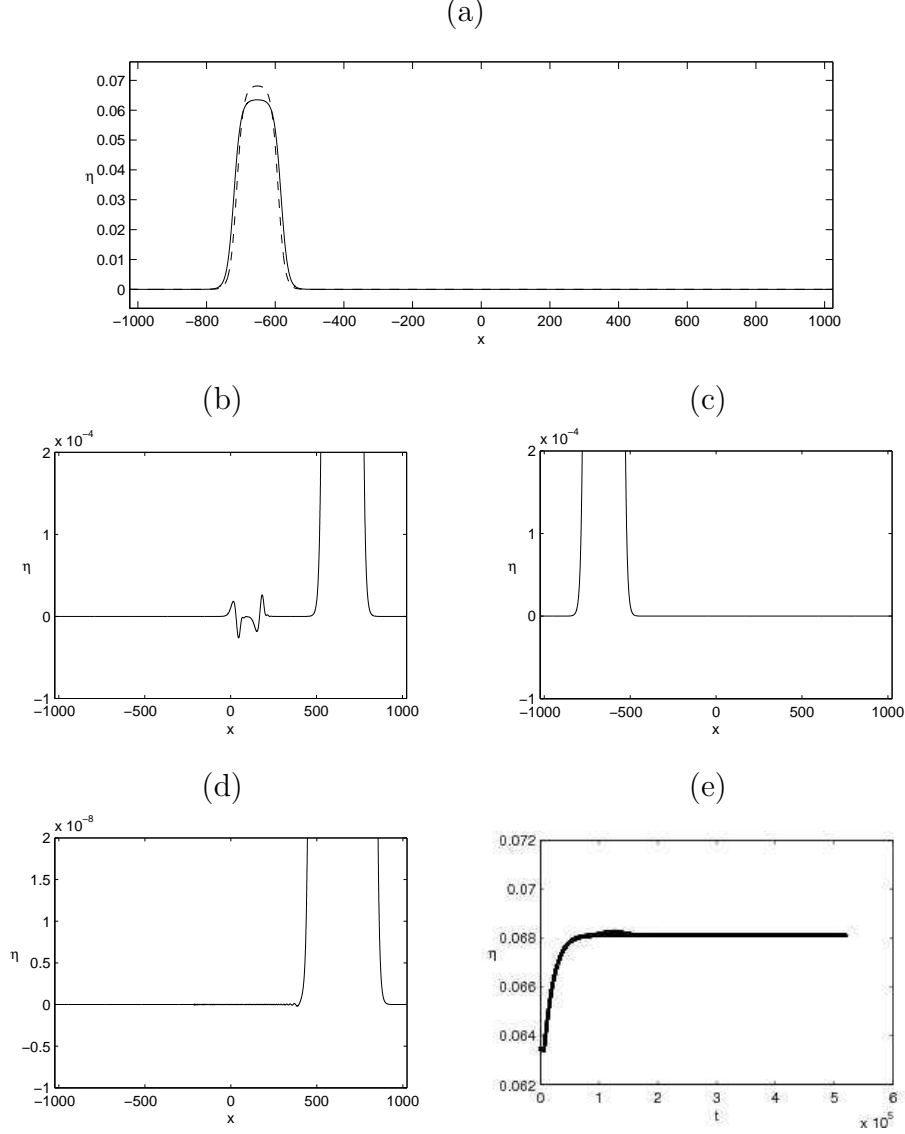


Fig. A.1. Flat solitary wave produced by iterative cleaning. This is a solution to the system of extended Boussinesq equations (47). (a) Difference in the profile before (solid line) and after (dashed line) cleaning. (b) Profile of the approximate solitary wave (51) after one propagation across the domain. (c) Profile (b) after cleaning and translation to the left of the domain. (d) Profile after several cleanings. Notice the change of scale in the vertical axis. (e) Evolution of the maximum amplitude η_{\max} as cleaning is repeated over and over. The amplitude reaches an asymptotic level.

in the previous case: indeed $\eta_{\max} = 0.10556057$ at collision, which is slightly larger than $0.06812113 + 0.03719492 = 0.10531605$. The phase shift is very small and the crest trajectory shows an interesting path. The overall conclusion is that run-ups and phase shifts are smaller for ‘table-top’ solitary waves than for ‘classical’ solitary waves.

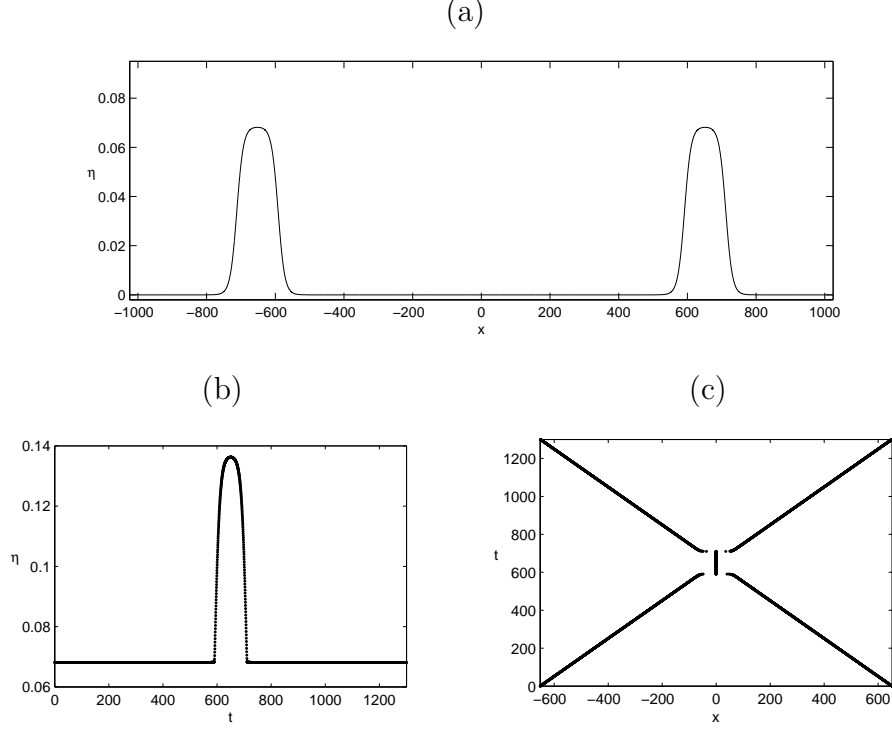


Fig. A.2. A collision between two clean ‘table-top’ solitary waves of equal height. This is a solution to the system of extended Boussinesq equations (47). (a) Initial profiles. (b) Time evolution of the amplitude η_{\max} . (c) Crest trajectory.

B Intermediate steps in the derivation of the extended Boussinesq system with cubic terms

Adding H times equation (26) to r times equation (27) yields

$$\begin{aligned}
& (r + H)\eta_t + H(w_x - rw'_x) + \alpha[(Hw + rw')\eta]_x \\
& + \frac{H}{2}\beta \left[(\theta^2 - \frac{1}{3})w_{xxx} - r(\theta'^2 - \frac{1}{3}H^2)w'_{xxx} \right] \\
& + \frac{1}{2}\alpha\beta \left[H(\theta^2 - 1)(\eta w_{xx})_x + r(\theta'^2 - H^2)(\eta w'_{xx})_x \right] \\
& + \frac{5H}{24}\beta^2 \left[\left(\theta^2 - \frac{1}{5} \right)^2 w_{xxxxx} - r \left(\theta'^2 - \frac{1}{5}H^2 \right)^2 w'_{xxxxx} \right] = 0.
\end{aligned} \tag{B.1}$$

Let us replace the variables w and w' in (B.1) by their expressions (42)-(43) in terms of W and let

$$F = \frac{1 + H}{r + H}, \quad G = H \frac{(\theta'^2 - \frac{1}{3}H^2) - (\theta^2 - \frac{1}{3})}{r + H}.$$

We consider all the terms one by one:

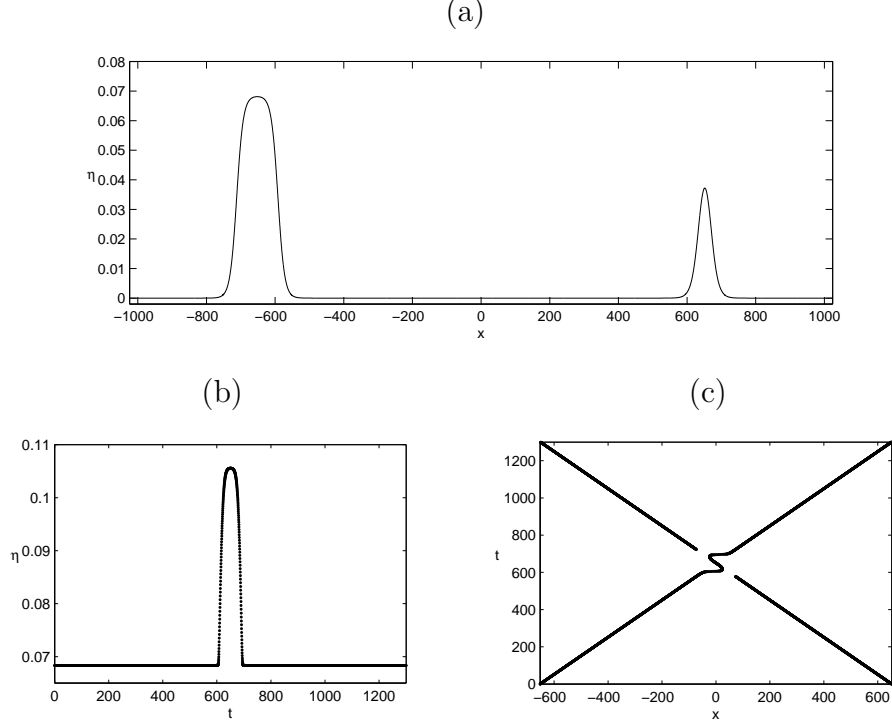


Fig. A.3. A collision between a clean solitary wave and a clean ‘table-top’ solitary wave. This is a solution to the system of extended Boussinesq equations (47). (a) Initial profiles. (b) Time evolution of the amplitude η_{\max} . (c) Crest trajectory.

(1) *Term* $H(w_x - rw'_x)$

$$H(w_x - rw'_x) = HW_x \quad (\text{B.2})$$

(2) *Term* $\alpha[(Hw + rw')\eta]_x$

From equation (42), we have

$$w - rw' = -(r + H)w' - \alpha FW\eta + \frac{1}{2}\beta GW_{xx},$$

so that

$$w' = -\frac{1}{r + H}W - \alpha\frac{1}{r + H}FW\eta + \frac{1}{2}\beta\frac{1}{r + H}GW_{xx}. \quad (\text{B.3})$$

Similarly from equation (43), we obtain

$$w = \frac{H}{r + H}W - \alpha\frac{r}{r + H}FW\eta + \frac{1}{2}\beta\frac{r}{r + H}GW_{xx}. \quad (\text{B.4})$$

Combining (B.3) and (B.4) yields

$$Hw + rw' = \frac{H^2 - r}{r + H}W - \alpha\frac{r(1 + H)}{r + H}FW\eta + \frac{1}{2}\beta\frac{r(1 + H)}{r + H}GW_{xx}.$$

Therefore

$$\begin{aligned}\alpha[(Hw + rw')\eta]_x &= \alpha \frac{H^2 - r}{r + H} (W\eta)_x - \alpha^2 \frac{r(1 + H)^2}{(r + H)^2} (W\eta^2)_x \\ &\quad + \frac{1}{2} \alpha \beta \frac{rH(1 + H) \left((\theta'^2 - \frac{1}{3}H^2) - (\theta^2 - \frac{1}{3}) \right)}{(r + H)^2} (W_{xx}\eta)_x.\end{aligned}$$

(3) *Term in w_{xxx} and w'_{xxx}*

Combining (B.3) and (B.4) yields

$$\begin{aligned}&\frac{H}{2} \beta \left[\left(\theta^2 - \frac{1}{3} \right) w_{xxx} - r \left(\theta'^2 - \frac{1}{3} H^2 \right) w'_{xxx} \right] \\ &= \frac{1}{2} \beta H \frac{H(\theta^2 - \frac{1}{3}) + r(\theta'^2 - \frac{1}{3} H^2)}{r + H} W_{xxx} \\ &\quad + \frac{1}{2} \alpha \beta r H (1 + H) \frac{\left(\theta'^2 - \frac{1}{3} H^2 \right) - \left(\theta^2 - \frac{1}{3} \right)}{(r + H)^2} (W\eta)_{xxx} \\ &\quad - \frac{1}{4} \beta^2 r H^2 \frac{\left((\theta'^2 - \frac{1}{3} H^2) - (\theta^2 - \frac{1}{3}) \right)^2}{(r + H)^2} W_{xxxxx}.\end{aligned}\tag{B.5}$$

(4) *Term in $(\eta w_{xx})_x$ and $(\eta w'_{xx})_x$*

Using (41) yields

$$\begin{aligned}&\frac{1}{2} \alpha \beta \left[H(\theta^2 - 1)(\eta w_{xx})_x + r(\theta'^2 - H^2)(\eta w'_{xx})_x \right] \\ &= \frac{1}{2} \alpha \beta \frac{H^2(\theta^2 - 1) - r(\theta'^2 - H^2)}{r + H} (\eta W_{xx})_x\end{aligned}\tag{B.6}$$

(5) *Term in w_{xxxxx} and w'_{xxxxx}*

Using (41) yields

$$\begin{aligned}&\frac{5}{24} H \beta^2 \left[\left(\theta^2 - \frac{1}{5} \right)^2 w_{xxxxx} - r \left(\theta'^2 - \frac{1}{5} H^2 \right)^2 w'_{xxxxx} \right] \\ &= \frac{5}{24} H \beta^2 \frac{H(\theta^2 - \frac{1}{5})^2 + r(\theta'^2 - \frac{1}{5} H^2)^2}{r + H} W_{xxxxx}\end{aligned}\tag{B.7}$$

Combining all terms (B.2)–(B.7) yields the first equation of the extended Boussinesq system

$$\begin{aligned}
& (r+H)\eta_t + HW_x + \alpha \frac{H^2 - r}{r+H} (W\eta)_x \\
& + \frac{1}{2}\beta \frac{H \left(H(\theta^2 - \frac{1}{3}) + r(\theta'^2 - \frac{1}{3}H^2) \right)}{r+H} W_{xxx} - \alpha^2 \frac{r(1+H)^2}{(r+H)^2} (W\eta^2)_x \\
& + \frac{1}{2}\alpha\beta \frac{rH(1+H)}{(r+H)^2} \left((\theta'^2 - \frac{1}{3}H^2) - (\theta^2 - \frac{1}{3}) \right) (W_{xx}\eta)_x \\
& + \frac{1}{2}\alpha\beta \frac{H^2(\theta^2 - 1) - r(\theta'^2 - H^2)}{r+H} (W_{xx}\eta)_x \\
& + \frac{1}{2}\alpha\beta rH(1+H) \frac{(\theta'^2 - \frac{1}{3}H^2) - (\theta^2 - \frac{1}{3})}{(r+H)^2} (W\eta)_{xxx} \\
& - \frac{1}{4}\beta^2 \frac{rH^2 \left((\theta'^2 - \frac{1}{3}H^2) - (\theta^2 - \frac{1}{3}) \right)^2}{(r+H)^2} W_{xxxxx} \\
& + \frac{5}{24}H\beta^2 \frac{H(\theta^2 - \frac{1}{5})^2 + r(\theta'^2 - \frac{1}{5}H^2)^2}{r+H} W_{xxxxx} = 0
\end{aligned} \tag{B.8}$$

We proceed the same way for equation (28).

(1) *Term in w_{xxt} and w'_{xxt}*

$$\begin{aligned}
& \frac{1}{2}\beta \left[(\theta^2 - 1)w - r(\theta'^2 - H^2)w' \right]_{xxt} = \\
& \frac{1}{2}\beta \frac{H(\theta^2 - 1) + r(\theta'^2 - H^2)}{r+H} W_{xxt} - \frac{1}{2}\alpha\beta \frac{r(1+H) \left((\theta^2 - 1) - (\theta'^2 - H^2) \right)}{(r+H)^2} (W\eta)_{xxt} \\
& + \frac{1}{4}\beta^2 \frac{rH \left((\theta^2 - 1) - (\theta'^2 - H^2) \right) \left((\theta'^2 - \frac{1}{3}H^2) - (\theta^2 - \frac{1}{3}) \right)}{(r+H)^2} W_{xxxxt}
\end{aligned} \tag{B.9}$$

(2) *Term $\alpha(w w_x - r w' w'_x)$*

$$\alpha(w w_x - r w' w'_x) = \alpha \frac{H^2 - r}{(r+H)^2} W W_x - \alpha^2 \frac{r(H+1)^2}{(r+H)^3} (W^2 \eta)_x$$

$$+\frac{1}{2}\alpha\beta\frac{rH(H+1)\left((\theta'^2-\frac{1}{3}H^2)-(\theta^2-\frac{1}{3})\right)}{(r+H)^3}(WW_{xx})_x \quad (\text{B.10})$$

(3) *Term*

$$\alpha\beta\left[(\eta w_{xt})_x + rH(\eta w'_{xt})_x\right] = \alpha\beta\frac{H(1-r)}{r+H}(\eta W_{xt})_x \quad (\text{B.11})$$

(4) *Term*

$$\frac{1}{2}\alpha\beta\left[(\theta^2-1)ww_{xxx} - r(\theta'^2-H^2)w'_xw'_{xxx}\right] = \frac{1}{2}\alpha\beta\frac{H^2(\theta^2-1)-r(\theta'^2-H^2)}{(r+H)^2}WW_{xxx} \quad (\text{B.12})$$

(5) *Term*

$$\frac{1}{2}\alpha\beta\left[(\theta^2+1)w_xw_{xx} - r(\theta'^2+H^2)w'_xw'_{xx}\right] = \frac{1}{2}\alpha\beta\frac{H^2(\theta^2+1)-r(\theta'^2+H^2)}{(r+H)^2}W_xW_{xxx} \quad (\text{B.13})$$

(6) *Term*

$$\begin{aligned} & \frac{1}{2}\beta^2\left((\theta^2-1)(5\theta^2-1)w_{xxxxt} - r(\theta'^2-H^2)(5\theta'^2-H^2)w'_{xxxxt}\right) \\ &= \frac{1}{2}\beta^2\frac{H(\theta^2-1)(5\theta^2-1)+r(\theta'^2-H^2)(5\theta'^2-H^2)}{r+H}W_{xxxxt} \end{aligned} \quad (\text{B.14})$$

Combining all terms (B.9)–(B.14) yields

$$\begin{aligned}
& (1-r)\eta_x + W_t + \alpha \frac{H^2 - r}{(r+H)^2} W W_x \\
& + \frac{1}{2} \beta \frac{H(\theta^2 - 1) + r(\theta'^2 - H^2)}{r+H} W_{xxt} - \alpha^2 \frac{r(1+H)^2}{(r+H)^3} (W^2 \eta)_x \\
& + \frac{1}{2} \alpha \beta \frac{rH(H+1) \left((\theta'^2 - \frac{1}{3}H^2) - (\theta^2 - \frac{1}{3}) \right)}{(r+H)^3} (W W_{xx})_x \\
& + \alpha \beta \frac{H(1-r)}{r+H} (\eta W_{xt})_x + \frac{1}{2} \alpha \beta \frac{H^2(\theta^2 - 1) - r(\theta'^2 - H^2)}{(r+H)^2} W W_{xxx} \\
& + \frac{1}{2} \alpha \beta \frac{H^2(\theta^2 + 1) - r(\theta'^2 + H^2)}{(r+H)^2} W_x W_{xx} \\
& - \frac{1}{2} \alpha \beta \frac{r(1+H) \left((\theta^2 - 1) - (\theta'^2 - H^2) \right)}{(r+H)^2} (W \eta)_{xxt} \\
& + \frac{1}{4} \beta^2 \frac{rH \left((\theta^2 - 1) - (\theta'^2 - H^2) \right) \left((\theta'^2 - \frac{1}{3}H^2) - (\theta^2 - \frac{1}{3}) \right)}{(r+H)^2} W_{xxxxt} \\
& + \frac{1}{2} \beta^2 \frac{H(\theta^2 - 1)(5\theta^2 - 1) + r(\theta'^2 - H^2)(5\theta'^2 - H^2)}{r+H} W_{xxxxt} = 0
\end{aligned} \tag{B.15}$$

References

- [1] D.S. Agafontsev, F. Dias, E.A. Kuznetsov, Deep-water internal solitary waves near critical density ratio, *Physica D* **225** (2007) 153–168.
- [2] R. Barros, S.L. Gavriluk, V.M. Teshukov, Dispersive nonlinear waves in two-layer flows with free surface. I. Model derivation and general properties, *Studies in Applied Mathematics* (2007), in press.
- [3] T.B. Benjamin, T.J. Bridges, Reappraisal of the Kelvin–Helmholtz problem. I. Hamiltonian structure, *J. Fluid Mech.* **333** (1997) 301–325.
- [4] J.L. Bona, M. Chen, A Boussinesq system for two-way propagation of nonlinear dispersive waves, *Physica D* **116** (1998) 417–430.

- [5] J.L. Bona, M. Chen, J.-C. Saut, Boussinesq equations and other systems for small-amplitude long waves in nonlinear dispersive media. I: Derivation and linear theory, *J. Nonlinear Sci.* **12** (2002) 283–318.
- [6] J.L. Bona, V.A. Dougalis, D.E. Mitsotakis, Numerical solution of KdV–KdV systems of Boussinesq equations. I. The numerical scheme and generalized solitary waves, *Mathematics and Computers in Simulation* **74** (2007) 214–228.
- [7] J.L. Bona, W.G. Pritchard, L.R. Scott, An evaluation of a model equation for water waves, *Phil. Trans. R. Soc. Lond. A* **302** (1981) 457–510.
- [8] T.J. Bridges, N.M. Donaldson, Reappraisal of criticality for two-layer flows and its role in the generation of internal solitary waves, *Phys. Fluids* (2007), to appear
- [9] W. Choi, R. Camassa, Fully nonlinear internal waves in a two-fluid system, *J. Fluid Mech.* **396** (1999) 1–36.
- [10] W. Craig, P. Guyenne, J. Hammack, D. Henderson, C. Sulem, Solitary water wave interactions, *Phys. Fluids* **18** (2006) 057106.
- [11] W. Craig, P. Guyenne, H. Kalisch, Hamiltonian long wave expansions for free surfaces and interfaces, *Comm. Pure Appl. Math.* **58** (2005) 1587–1641.
- [12] F. Dias, T. Bridges, Geometric aspects of spatially periodic interfacial waves, *Stud. Appl. Math.* **93** (1994) 93–132.
- [13] F. Dias, J.-M. Vanden-Broeck, On internal fronts, *J. Fluid Mech.* **479** (2003) 145–154.
- [14] F. Dias, J.-M. Vanden-Broeck, Two-layer hydraulic falls over an obstacle, *Europ. J. Mech. B/Fluids* **23** (2004) 879–898.
- [15] V.A. Dougalis, D.E. Mitsotakis, Solitary waves of the Bona-Smith system, *Advances in scattering theory and biomedical engineering*, ed. by D. Fotiadis and C. Massalas, World Scientific, New Jersey, (2004), pp. 286–294.
- [16] W.A.B. Evans, M.J. Ford, An integral equation approach to internal (2-layer) solitary waves, *Phys. Fluids* **8** (1996) 2032–2047.
- [17] C. Fochesato, F. Dias, R. Grimshaw, Generalized solitary waves and fronts in coupled Korteweg–de Vries systems, *Physica D* **210** (2005) 96–117.
- [18] M. Funakoshi, M. Oikawa, Long internal waves of large amplitude in a two-layer fluid, *J. Phys. Soc. Japan* **55** (1986) 128–144.
- [19] R. Grimshaw, D. Pelinovsky, E. Pelinovsky, A. Slunyaev, Generation of large-amplitude solitons in the extended Kortewegde Vries equation, *Chaos* **12** (2002) 1070–1076.
- [20] K.R. Helfrich, W.K. Melville, Long nonlinear internal waves, *Annu. Rev. Fluid Mech.* **38** (2006) 395–425.

- [21] T. Kataoka, The stability of finite-amplitude interfacial solitary waves, *Fluid Dynamics Research* **38** (2006) 831–867.
- [22] O. Laget, F. Dias, Numerical computation of capillary-gravity interfacial solitary waves, *J. Fluid Mech.* **349** (1997) 221–251.
- [23] H. Michallet, E. Barthélemy, Experimental study of interfacial solitary waves, *J. Fluid Mech.* **366** (1998) 159–177.